

# Mapping Firms' Locations in Technological Space: A Topological Analysis of Patent Statistics\*

Emerson G. Escobar<sup>†</sup> Yasuaki Hiraoka<sup>‡</sup> Mitsuru Igami<sup>§</sup> Yasin Ozcan<sup>¶</sup>

October 13, 2021

## Abstract

Where do firms innovate? Mapping their locations and directions in technological space is challenging due to its high dimensionality. We propose a new method to characterize firms' inventive activities via topological data analysis (TDA) that represents high-dimensional data in a shape graph. Applying this method to 333 major firms' patents in 1976–2005 reveals substantial heterogeneity: some firms remain undifferentiated; others develop unique portfolios. Firms with unique trajectories, which we define graph-theoretically as “flares” in the Mapper graph, perform better. This association is statistically and economically significant, and continues to hold after we control for portfolio size and firm survivorship. We then compare our approach with existing techniques to further demonstrate its use in data visualization and exploration.

*Keywords:* Innovation, Mapper, Patents, R&D, Topological data analysis.

*Journal of Economic Literature (JEL) classifications:* C65, C88, L10, O30.

---

\*First version: August 31, 2019 (<https://arxiv.org/abs/1909.00257v1>). For helpful comments, we thank Susan Athey, Iain Cockburn, Marek Giebel, David Hsu, Adam Jaffe, and Yihan Yan, as well as participants at Yale IO Seminar, the 2019 *NBER Innovation Information Initiative* meeting, *Joint Conference on Applied Mathematics 2019* by the Mathematical Society of Japan (MSJ), *MSJ Spring Meeting 2020*, Kyoto University Applied Mathematics Seminar, *TDA for Applications - Tutorial & Workshop* at Tohoku University, the 2020 *Econometric Society World Congress* at Bocconi University, the Hong Kong University of Science and Technology, *TopoNets 2020*, the *MaCCI/EPoS Conference on Innovation*, the 2021 *International Industrial Organization Conference*, and KU Leuven *Data & Algorithms for ST&I Studies* conference. We thank Alan Chiang and Chise Igami for research assistance.

<sup>†</sup>Kobe University Graduate School of Human Development and Environment, and RIKEN Center for Advanced Intelligence Project. E-mail: e.g.escolar@people.kobe-u.ac.jp.

<sup>‡</sup>WPI-ASHBi, Kyoto University Institute for Advanced Study, Kyoto University and Center for Advanced Intelligence Project, RIKEN. E-mail: hiraoka.yasuaki.6z@kyoto-u.ac.jp.

<sup>§</sup>Yale Department of Economics. E-mail: mitsuru.igami@yale.edu.

<sup>¶</sup>FTI Consulting. Email: ozcan@alum.mit.edu.

# 1 Introduction

The “rate and direction of inventive activity” have been recognized as one of the main themes in economics since at least the conference of the same title in 1960 (Nelson (1962), Lerner and Stern (2012)). Whereas the rate of innovation has been studied extensively, research on its direction has seen much less progress. Nevertheless, recent studies suggest the direction of scientific change is both an important choice for individual researchers and a critical outcome for scientific communities (Azoulay, Fons-Rosen, and Graff Zivin (2019), Myers (2020)). These observations, along with the central role of product differentiation in the theory of industrial organization (IO), suggest the direction of inventive activity is important for firms and industries as well.

However, mapping the locations and directions of firms’ research and development (R&D) activities is a challenging problem because technological space has many dimensions, unlike physical/geographical space.<sup>1</sup> Even a relatively “coarse” classification system by the US Patent and Trademark Office (USPTO) uses more than 400 categories (patent classes), and large firms frequently conduct R&D in more than 100 classes, obtaining thousands of patents each year. As a result, the dimensionality of the action/state space is extremely high, and infinitely many directions of inventive activity are possible in principle. Modeling something we cannot even visualize and describe is difficult. Hence, before we can hope to model firms’ strategies in the technological space and understand their causal relationships with market outcomes such as profits and social welfare, developing a method for faithfully mapping their technological positions and documenting empirical regularities (i.e., measurement and exploratory data analysis) would be a crucial step.

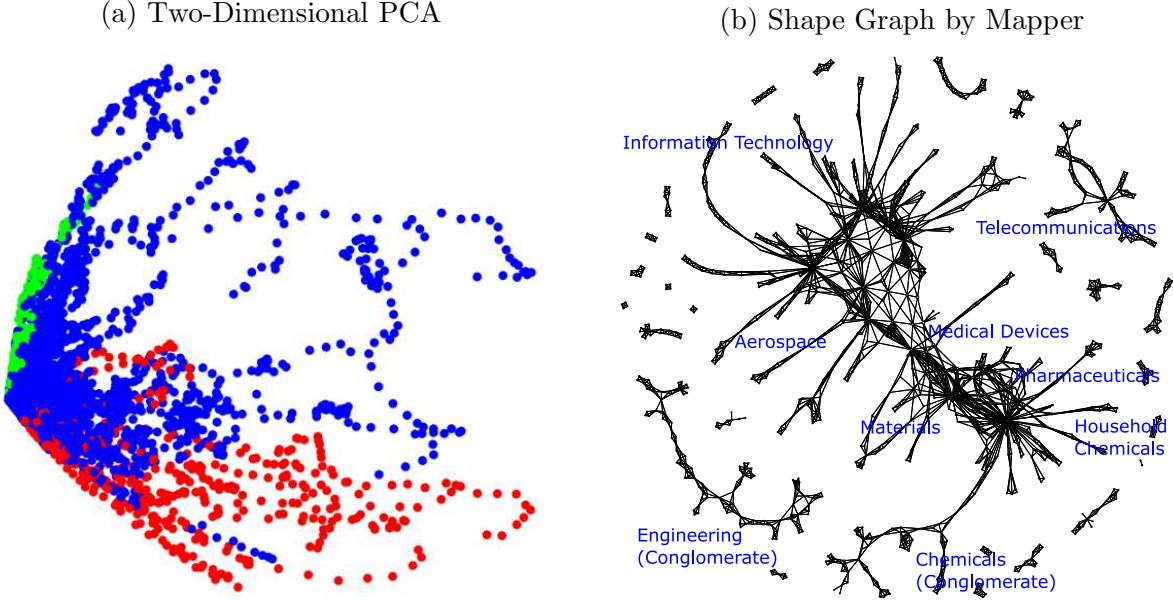
Given the high dimensionality of the problem, some dimensionality reduction is clearly needed. Commonly used methods include principal component analysis (PCA), multi-dimensional scaling (MDS), and various algorithms for clustering (e.g., k-means clustering). However, even though these existing methods provide some simplified visualization and description, fundamental issues remain unresolved: collapsing data would eliminate useful information about the direction of inventive activity. For example, Figure 1 (a) shows a PCA that projects onto a two-dimensional plane 333 major firms’ patent portfolios (vectors of logged patent counts across 430 USPTO classes) in 1976–2005. It visualizes the data and shows some patterns. For instance, huge clusters of points on the left side would seem to suggest many firms conduct R&D in close proximity, but this “densely populated area”

---

<sup>1</sup>Whereas a large literature exists on the geography of innovation (pioneered by Jaffe, Trajtenberg, and Henderson (1993)), relatively few papers explore technological space, because of methodological challenges.

could partly be an artifact of collapsing the other 428 dimensions.<sup>2</sup> Similar issues arise in other existing methods, due to information loss (see section 6 for an example of clustering). Thus, a faithful representation of the positions and directions of R&D requires new descriptive tools that avoid arbitrarily collapsing data, provide intuitive visualizations of how firms' patent portfolios evolve over time, and permit quantification of these dynamics.

Figure 1: Firms' Locations in Technological Space, 1976–2005



*Note:* Both pictures represent the evolution of 333 major firms' portfolios of US patents that are acquired by in-house R&D between 1976 and 2005. Each firm-year is a vector of log patent counts across 430 technological classes. The left panel is a two-dimensional PCA (red markers are IT firms, green markers are drug makers, and blue markers are all others). See Appendix Figure 8 for a three-dimensional PCA. The right panel is a Mapper graph based on the same data (see sections 3 and 4 for details).

This paper presents such a new method to represent firms' locations as a combinatorial/topological object (shape graph), which can be easily visualized and quantified in a variety of ways using graph theory. We adapt and extend a tool from computational topology called the Mapper procedure (Singh, Mémoli, and Carlsson, 2007). This algorithm is well founded on mathematical concepts from computational topology and geometry, such as the Reeb graph, and aims to preserve the topological and geometric information of the original data, in two steps. First, it clusters data points in each local neighborhood based on a distance metric of one's choice (e.g., cosine distance). Second, it connects clusters with edges if a pair of clusters shares at least one data point. Hence, even though the resulting

<sup>2</sup>See Appendix Figure 8 for a three-dimensional PCA, which is slightly more informative than the two-dimensional PCA. Note the other 427 dimensions are still missing.

graph might appear to visualize data on a two-dimensional plane—see Figure 1 (b)—as in the PCA plot, the shape graph retains the notions of proximity and continuity (in the original space) with edges between neighboring nodes.

We apply this method to the dynamic evolution of the 333 major firms’ patent portfolios across 430 USPTO classes in 1976–2005, and report three sets of results. First, we visualize these firms’ technological positions and their evolution over the three decades. Whereas “data visualization” plays only a minor role in most empirical studies, it embodies one of the main results in our context, because the systematic mapping of technological space is the central empirical problem that this paper addresses. We find many engineering firms remain undifferentiated and cluster together in the densely populated “trunk” or the “continental” part of the map. However, a few dozen firms, primarily in the information technology (IT) sector, start differentiating from the rest in the 1980s and the 1990s, developing unique portfolios and exhibiting distinctive trajectories, as represented by long “branches” or “flares” that spike out of the main trunk. In the topological space, which is coordinate free, these shapes and their time evolution provide explicit signatures of the unique “directions” of inventive activity.

Second, we propose a formal definition of such flares based on graph theory, as well as a computational method to measure their length, which suggests 40.3 % of the firms in our data exhibit some flares. We assess the empirical relevance of this “uniqueness” measure by following a traditional approach in the economics of innovation, such as Pakes and Griliches (1984) and Hall, Jaffe, and Trajtenberg (2005), which is to evaluate its statistical relationships with the firms’ financial performances (revenue, profit, and market value). Regression results suggest positive correlations between the flare length and the performance metrics. This association is statistically significant at conventional levels, and economically significant in magnitude (e.g., an extra length of flare in 1976–2005 is associated with 31%–40% higher performances as of 2005). Moreover, these patterns continue to hold (i) within each sector and industry, (ii) after controlling for portfolio size (i.e., total patent count), and (iii) in balanced-panel subsamples (i.e., after controlling for firm survivorship).

Third, we further investigate how our method compares with that of Jaffe (1989), which is based on k-means clustering and is one of the most prominent methods to study firms’ locations in the technological space. Our method differs from Jaffe’s in two ways: data-transformation protocol (logs vs. shares) and the scope of clustering (local vs. global). The first difference is trivial in the sense that we can use his protocol within our scheme as well, but the second is more fundamental. Whereas Jaffe’s global clustering is essentially a big

*discretization* operation that generates a list of disjoint clusters of firms, ours is designed to retain and recover the *continuum* of firms and industries in the original data. Using Jaffe’s measure within our method, we show that seemingly unrelated industries are in fact connected in the technological space, sometimes in surprising ways.

Thus, our approach is complementary to the existing methods and can generate new insights that are difficult to obtain otherwise. It helps us answer some of the most basic questions, including where firms innovate, how industries and technologies are connected, and how firms’ patent portfolios evolve over time.

We organize the rest of the paper as follows. The remainder of section 1 provides the literature context in economics. Section 2 introduces the idea of topological data analysis (TDA) and explains our method. Section 3 explains the data. Section 4 presents our first main result: a map of technological space that visualizes and describes the evolution of firms’ inventive activities over time. Section 5 reports our second result: measurement of flare length and its correlation with firms’ performances. Finally, section 6 presents an alternative version of the Mapper graph based on Jaffe’s protocol, and compares and contrasts it with his method. Section 7 concludes.

**Related Literature in Economics** Methodologically, we study the problem of characterizing firms’ behavior/status in a high-dimensional space (i.e., when the dimensionality of the action/state space is large). Exploratory data analysis (EDA) is a well developed idea in statistics to summarize the characteristics of datasets since at least Tukey (1977), and is more recently rebranded as part of machine learning. As such, this paper fits into the growing literature that introduces novel techniques from mathematics, statistics, and computer science to analyze high-dimensional data.<sup>3</sup> The distinguishing feature of our paper from the rest of EDA and the “machine learning in economics” literature is the use of TDA. In fact, to our knowledge, this paper is the first in economics to apply and extend TDA methods in general, and the Mapper algorithm in particular.<sup>4</sup> We explain TDA and its literature in section 2.

Substantively, this paper builds on and contributes to IO and the economics of innovation

---

<sup>3</sup>For surveys and examples, see Belloni, Chernozhukov, and Hansen (2014), Varian (2014), Athey and Imbens (2017), Brumm and Scheidegger (2017), Chernozhukov et al. (2018), Cattaneo, Jansson, and Ma (2019), Gentzkow, Kelly, and Taddy (2019), Iskhakov, Rust, and Schjerning (2020), and Igami (2020).

<sup>4</sup>To be precise, we are aware of several applications of TDA to financial time series (Gidea (2017), Gidea and Katz (2018), Guo et al. (2020), Goel, Pasricha, and Mehra (2020), Majumdar and Laha (2020), Qiu, Rudkin, and Dłotko (2020)). However, they are relatively short papers primarily by non-economists and published in either computer science or physics journals, with limited connections to economics.

in general, and the empirical analysis of R&D, patents, and firm performance in particular. The literature is too large to summarize here; see Griliches (1990) for an overview of patent statistics as an indicator of innovation, and Cohen (2010), Nagaoka, Motohashi, and Goto (2010), and Lerner and Seru (2017) for surveys. Despite well-known limitations,<sup>5</sup> patent statistics remain one of the most systematic sources of information on inventive activities, and continue to play a central role in the economics of innovation.<sup>6</sup> The most closely related work to ours is Jaffe (1989), who pioneered the use of patent-class information to characterize firms' positions, and is therefore a direct predecessor of this paper. The literature has continued to use both his distance metric and his clustering algorithm (cosine distance and k-means clustering, respectively).<sup>7</sup>

Finally, this paper also contributes to the rapidly growing literature that applies “big data” techniques to patents. Because patents are fundamentally legal documents, researchers are introducing a range of modern tools from computational linguistics to conduct text analysis (e.g., Bryan and Ozcan (2016), Kuhn, Younge, and Marco (2020), Myers and Lanahan (2020)).<sup>8</sup> Whereas these papers focus on (i) converting text in the original documents into high-dimensional numerical data and (ii) proposing dissimilarity measures between patents, our method takes any kinds of (i) and (ii)—text-based or not—as given, and (iii) aims to faithfully represent the shape of such “big data,” in a form that permits visualization and further analysis. Thus, our proposal is complementary to both Jaffe’s traditional framework and more recent (e.g., text-based) approaches.

---

<sup>5</sup>For example, see Griliches (1990), Lerner and Seru (2017), and Igami and Subrahmanyam (2019).

<sup>6</sup>Recent micro-econometric publications at top economics journals that use patents include Cockburn, Lanjouw, and Schankerman (2016), Howell (2017), Azoulay, Fons-Rosen, and Graff Zivin (2019), and Sampat and Williams (2019), among many others. A major data-cleaning project is undertaken by Arora, Belenzon, and Sheer (2019), who extend the NBER patent database of Hall, Jaffe, and Trajtenberg (2001) and Bessen (2009) to 2015, linking firm names to the Compustat financial data. Since December 2019, such efforts to construct and improve patent-based innovation metrics have been renewed and coordinated under the *NBER Innovation Information Initiative* organized by Adam Jaffe.

<sup>7</sup>For example, Bloom, Schankerman, and Van Reenen (2013) present a sophisticated version of Jaffe’s (1986) study of R&D spillovers. Moser and San (2020) use k-means clustering to simplify the areas of science. Benner and Waldfogel (2008) scrutinize the USPTO’s classification procedures, investigate statistical biases in the analysis of patent-class data, and offer practical suggestions. Bar and Leiponen (2012) propose a new distance metric, called the min-complement distance, which satisfies a desirable property (independence of irrelevant patent classes) that no other conventional measures satisfy.

<sup>8</sup>Similarly, Hoberg and Phillips (2016) use text analysis on firms’ Form 10-K product descriptions to describe and characterize product-market competition.

## 2 Method

This section explains the idea of TDA, the Mapper algorithm, our specifications, and our original method for detecting and measuring flares.

### 2.1 Brief Introduction to TDA

Most data-analysis techniques in economics and elsewhere concern the evaluation of parameters or other quantities that characterize the system (the data-generating process, or DGP).<sup>9</sup> However, not all aspects of a system are readily summarized by numerical quantities. In particular, the “shape” of the data (i.e., the properties that remain invariant under “stretching” and “shrinking,” e.g., loops and branching patterns) could constitute a significant insight about real phenomena.

Shape is a somewhat nebulous concept and may appear too intuitive to define precisely and describe quantitatively, but the unique strength of TDA is its ability to capture and summarize such information in a useful, small representation of the data. Even though it is not among the usual tools for empirical economists, topology as an area of pure mathematics has existed for more than a century, and provides a theoretical foundation for the analysis of shapes. The adaptation of topological techniques to real data has been undertaken only recently (Edelsbrunner, Letscher, and Zomorodian (2000), Zomorodian and Carlsson (2005), Carlsson (2009), Edelsbrunner and Harer (2010)). Nevertheless, TDA has already been successfully applied to an increasing number of fields, including biology, chemistry, and materials science (e.g., Nicolau, Levine, and Carlsson (2011), Hiraoka et al. (2016)). See Chazal and Michel (2017) for a brief introduction.

Among the techniques in TDA, the study of persistent homology has emerged as the most popular.<sup>10</sup> However, its application to high-dimensional data is constrained by the computational cost of constructing combinatorial models (e.g., Čech complex, Alpha complex, Rips complex, etc.), which requires one to check higher-order intersections of the balls in that space and to store all the information. Various methods have been proposed to address this “curse of dimensionality,” but persistent homology can handle only tens of dimensions in

---

<sup>9</sup>This and the next paragraphs borrow expositions from Epstein, Carlsson, and Edelsbrunner (2011) and Sizemore et al. (2019).

<sup>10</sup>Epstein, Carlsson, and Edelsbrunner (2011) explain the popularity of homology groups by pointing out that they offer an attractive combination of strong explanatory power, a clear intuitive meaning, and a low computational cost. Because the notion of shape within (finite) datasets is inevitably stochastic, and because homology is sensitive to noise in the data, *persistent* homology is used to quantify the stability of geometric features with respect to perturbations, so that real phenomena could be distinguished from artifacts of noise.

the current state of the art. By contrast, Mapper can easily handle thousands and even millions of dimensions, by focusing on the global topology of the data and providing simplified representations of their shape via nonlinear transformations.<sup>11</sup> Thus, whereas persistent homology offers a fine-grained characterization of cavities in relatively low-dimensional data, Mapper enables a relatively coarse characterization of *very* high-dimensional data, which makes it particularly suitable for our empirical context.

Since Singh, Mémoli, and Carlsson (2007) introduced Mapper, it has been applied to study an RNA folding pathway (Yao et al., 2009), the DNA microarray data of breast cancer (Nicolau, Levine, and Carlsson, 2011), cellular differentiation and development (Rizvi et al., 2017), and the organization of whole-brain activity maps (Saggar et al., 2018). Methodologically, Lum et al. (2013) is the most closely related work to ours, because they also propose a flare-detection algorithm. Their method uses global graph-theoretic properties that are applicable to any graph, without using any additional information from the Mapper algorithm.<sup>12</sup> By contrast, our algorithm takes advantage of particularities of our Mapper graph, where each node is a set of firm-years. We ensure each flare that we identify is associated with a specific firm. Hence, it can be interpreted as *a flare of that firm*.

## 2.2 The Mapper Algorithm

We provide a quick review of the Mapper method introduced by Singh, Mémoli, and Carlsson (2007). Given some complicated and high-dimensional data, Mapper provides a simplified representation of the data via a graph that captures some of its important “topological features” such as branching, flares, and islands.

We assume the data are given as a set of points  $X$  together with a dissimilarity function  $\delta : X \times X \rightarrow \mathbb{R}_{\geq 0}$ . The Mapper graph is constructed in four steps.

1. Project  $X$  into  $\mathbb{R}^d$  by some filter function  $f : X \rightarrow \mathbb{R}^d$ .
2. Cover the image  $f(X)$  using an overlapping cover  $\mathcal{C} = \{C_j\}_{j=1}^J$ .
3. For each cover element  $C_j$ , apply some clustering algorithm to its pre-image  $f^{-1}(C_j)$  based on the dissimilarity function  $\delta$  to obtain a partition of  $f^{-1}(C_j)$  into  $K_j$  clusters,

---

<sup>11</sup>For example, Rizvi et al. (2017) use Mapper to study single-cell gene expression, where the number of dimensions equals the number of expressed genes (up to 10,000).

<sup>12</sup>Specifically, their flare detection algorithm uses the 0-dimensional persistent homology (Edelsbrunner, Letscher, and Zomorodian, 2000) of the graph filtered by an eccentricity measure on its nodes. An eccentricity measure tends to give a higher value to nodes that are “eccentric” (on tips of flares) compared to central nodes (on the trunks).

$V_{j,k}$  ( $k = 1, \dots, K_j$ ):<sup>13</sup>

$$f^{-1}(C_j) = \bigsqcup_{k=1}^{K_j} V_{j,k}. \quad (1)$$

4. Construct the graph  $G$  with nodes (vertices) consisting of all  $V_{j,k}$ s. Connect two nodes,  $V_{j,k}$  and  $V_{j',k'}$ , by an edge if  $V_{j,k} \cap V_{j',k'} \neq \emptyset$ .

Figure 2: Illustration of the Mapper Procedure

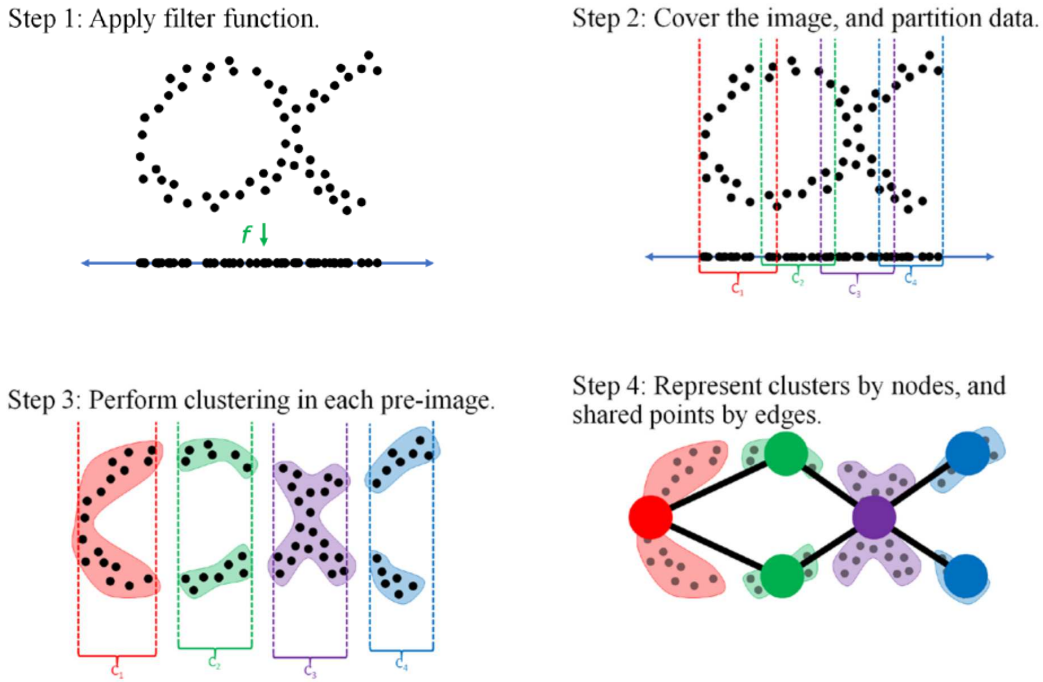


Figure 2 illustrates this procedure with an example. Let us start with data  $X$  given by the points in two-dimensional space. Our goal is to obtain a simplified representation of  $X$  while preserving its topological features, such as holes and branches. In step 1, we project  $X$  onto the horizontal axis (i.e.,  $d = 1$ ). This operation reduces the dimensionality of the data by eliminating the second dimension (i.e., information on the vertical axis in this case). In step 2, we cover these points on the horizontal axis by four equal-sized intervals (i.e., cover elements)  $C_1, C_2, C_3$ , and  $C_4$  (i.e.,  $J = 4$ ) with overlaps.<sup>14</sup> In step 3, we look at each interval  $C_j$ , and cluster adjacent points *in the original data space* with two dimensions. In step 4, we

<sup>13</sup>The notation  $\sqcup$  represents a disjoint union.

<sup>14</sup>The degree of overlap is approximately 20% in the pictured example. The analyst can alter it (see section 2.3).

represent these clusters by nodes, and connect them with edges whenever adjacent clusters share the same points within their overlapping regions.

The resulting graph is much simpler than the original data and amenable to graph-theoretic analyses, but it still preserves the “global structure” of  $X$  (i.e., topological features that span multiple local regions, such as loops and long branches/flares). By contrast, using conventional techniques for dimensionality reduction alone would be similar to performing only step 1. Likewise, directly performing clustering in the original data would be the same as skipping steps 1 and 2, which would probably generate a single big cluster for the entire data in this case. Neither approach would be able to recover the *shape* of the data (i.e., a collection of global structures). For this particular example, the usefulness of the Mapper graph is limited, as the original data itself is only two-dimensional and can be readily visualized. However, for more complicated high-dimensional data, a simplified graph representation offers a helpful visual aid.

One way to interpret the Mapper procedure is to view it as a kind of local clustering together with “global reconstruction” (i.e., replication of global structures). The choice of the filter function and cover determines the local regions  $f^{-1}(U_j) \subset X$  of the data. Then, the clustering algorithm is applied only locally, to each local region. The construction of the graph  $G$  recovers some of the global information by connecting nodes (each of which is a cluster of points in  $X$ ) whenever they share points in the original data.

### 2.3 Application of Mapper to Our Data

Recall that our data are a panel of 333 firms’ yearly patent applications (and/or acquisitions) across 430 technology classes between the years 1976 and 2005.<sup>15</sup> For each firm  $i$ , each year  $t$ , and each patent class  $c$ , we have patent count  $p_{i,t,c}$ . We regard each firm-year as a single observation represented by a vector  $p_{i,t} \in \mathbb{R}^{430}$ . Hence, each firm-year is a point  $p_{i,t}$  in the 430-dimensional technology space.

Firms’ patent applications in any single year tend to be volatile and less representative of their underlying R&D activities. This issue is particularly important in the use of patent-class data, as Benner and Waldfogel (2008) point out. We follow their recommendation to smooth out yearly fluctuations by using a five-year moving window:

$$\tilde{p}_{i,t} = p_{i,t} + p_{i,t+1} + \dots + p_{i,t+4}. \quad (2)$$

---

<sup>15</sup>Section 3 explains the data more thoroughly, including their sources and summary statistics.

Another practical consideration is the highly skewed distribution of patent count, which we explain in section 3. We address this issue by applying a logarithmic transform,<sup>16</sup>

$$\tilde{p}_{i,t} \mapsto \ln(\tilde{p}_{i,t} + 1) =: x_{i,t}. \quad (3)$$

Let  $X = \{x_{i,t}\}$  be the point cloud consisting of the transformed data. We use the following specifications in constructing a mapper graph for  $X$ . We use the Python implementation, KeplerMapper, by Van Veen and Saul (2019).

1. The filter function is  $f : X \rightarrow \mathbb{R}^2$ , which projects  $X$  to its first two principal axes as obtained by PCA.<sup>17</sup>
2. For the cover of the image of  $f$ , we use the default cover implementation in KeplerMapper. We set the resolution level (called the “number of cubes,”  $n$ ) to 20 in our baseline specification, and the degree of overlap,  $o$ , to 50%, which creates a  $20 \times 20$  grid of overlapping squares.<sup>18</sup>
3. For the clustering algorithm, we use single-linkage clustering together with the heuristic as proposed by Singh, Mémoli, and Carlsson (2007) for choosing the number of clusters.

For the dissimilarity measure between points in  $X$ , we use the cosine distance in our baseline specification, because it is the most commonly used one in the innovation literature,

$$\delta(x_{i,t}, x_{i',t'}) = 1 - \frac{\sum_c x_{i,t,c} x_{i',t',c}}{\sqrt{\sum_c x_{i,t,c}^2} \sqrt{\sum_c x_{i',t',c}^2}}, \quad (4)$$

where  $\delta(x_{i,t}, x_{i',t'})$  is the distance between firm-years  $(i, t)$  and  $(i', t')$ , and  $x_{i,t,c}$  is firm-year  $(i, t)$ ’s patent count in class  $c$  in the transformed data.<sup>19</sup>

---

<sup>16</sup>We use an alternative data-transformation protocol (calculating shares of classes within each firm-year) in section 6, in which we compare our method with Jaffe’s (1989).

<sup>17</sup>Note we use PCA only for the purpose of determining local regions. The subsequent clustering is performed in each pre-image in the original space and *not* in the PCA space.

<sup>18</sup>We set  $n$  to 15 and 25, and  $o$  to 30%, in sensitivity analysis, which result in qualitatively similar Mapper graphs. These choices are based on the following practical considerations. Lower resolution levels ( $n$ ) lead to Mapper graphs that are too simple and coarse to reveal interesting structures in the data; higher values of  $n$  lead to more detailed outputs that are computationally more difficult to render and navigate. Similarly, lower degrees of overlap ( $o$ ) lead to graphs without much connectivity to study; higher values of  $o$  lead to too many trivial connections that increase computational burden without additional insights.

<sup>19</sup>As a sensitivity analysis, we also use other distance measures, including Euclidean, correlation, min-complement, and Mahalanobis. The results are broadly similar (see Appendix).

## 2.4 Detection of Flares

As section 2.2 explained, Mapper provides a simplified representation of complicated data via a graph  $G$  that captures some of its more important topological features. In this section, we discuss the detection of one such feature: flares.

Let us review some basic concepts from graph theory. In general, a *graph*  $G = (V, E)$  is a set  $V$  of nodes (vertices) and a set  $E$  of edges. We assume that each edge  $e \in E$  of  $G$  is assigned the weight  $w(e) = 1$ .<sup>20</sup> For  $u, v \in G$ , the *length*  $\ell(p)$  of a path  $p$  from  $u$  to  $v$  is the sum of the weights of the edges of  $p$ . The *distance*  $d_G(u, v)$  between  $u$  and  $v$  is the minimum length of all paths  $p$  in  $G$  from  $u$  to  $v$ . For simplicity, we write  $d(u, v)$  for  $d_G(u, v)$ .

For a graph  $G$  and a subset  $V'$  of the nodes of  $G$ , the *full subgraph* of  $G$  with nodes  $V'$ , denoted by  $G[V']$ , is the graph with the set of nodes  $V'$  and edges consisting of all edges of  $G$  whose endpoints are both in  $V'$ . It is the maximal subgraph of  $G$  with set of nodes  $V'$ .

**Definition 1** (Ball). Let  $r \in \mathbb{R}$  and  $u \in G$ . The (closed) ball  $B_r(u)$  in  $G$  is

$$B_r(u) = G[\{v \in G \mid d(u, v) \leq r\}].$$

In words, it is the full subgraph of  $G$  of all nodes at most distance  $r$  from  $u$ .

Now, consider a graph  $G = (V, E)$  obtained from the Mapper algorithm applied to our data. From the construction of the Mapper graph, each node  $v \in V$  will consist of points (firm-years) of the form  $x_{i,t}$ . To simplify, we adopt the following notation, because we want to consider firms and not firm-years for the analysis.

**Notation 2.** In the setting above, firm  $i$  is said to be in node  $v$ , or, equivalently,  $v$  contains firm  $i$  if node  $v$  contains an observation of firm  $i$  at some time  $t$ , that is,  $x_{i,t} \in v$  for some  $t$ . In this situation, we write  $i \in v$ .

For each firm  $i$ , we want to determine whether  $i$  appears as a flare in  $G$ . One way to extract flares is to use global graph-theoretic properties of  $G$ , as in the method proposed in Lum et al. (2013) using 0-persistence of eccentricity (or centrality). Instead, we start with the requirement that we only consider a structure to be a “flare of  $i$ ” if each node in the flare contains  $i$ . This way, we focus on a smaller graph  $G_i$  defined below, which contains only nodes that involve  $i$ , and look for flares therein.<sup>21</sup> We see later that this perspective simplifies computations.

---

<sup>20</sup>The theory can be extended to handle positive weights  $w(e) > 0$  that are different across edges.

<sup>21</sup>More generally, one may consider a flare that involves multiple firms. We restrict our attention to single-firm flares in this paper because they are the most salient feature of our Mapper graphs.

**Definition 3** (Induced subgraph  $G_i$  of firm  $i$ ). Let  $i$  be a firm. Define  $G_i$  to be

$$G_i = G[\{v \in G \mid i \in v\}].$$

That is,  $G_i$  is the full subgraph of  $G$  formed by nodes that contain firm  $i$ . We decompose the nodes of  $G_i$  into “interior” and “boundary.”

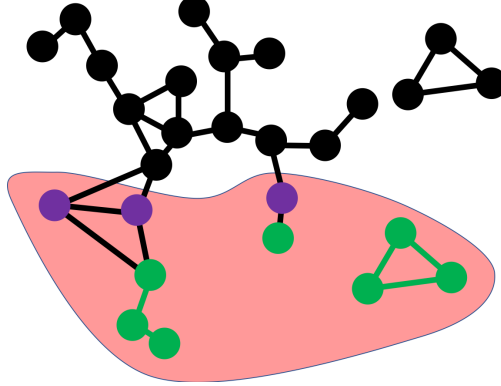
**Definition 4** (Interior and boundary of  $G_i$ ).

1. The *interior*  $F_i$  of  $i$  in  $G$  is defined to be  $F_i = G[\{v \in G_i \mid B_1(v) \subseteq G_i\}]$ .
2. The *boundary* of  $i$  in  $G$  is  $G_i \setminus F_i$ .

In words, the interior  $F_i$  contains all nodes  $v$  of  $G_i$  such that  $G_i$  contains all neighbors of  $v$  (i.e., the ball of radius 1 around  $v$ ). Lemma 12 in the Appendix shows that the boundary  $G_i \setminus F_i$  indeed serves as a “boundary” for  $F_i$ : to get outside of  $G_i$ , one always needs to go through the boundary.

Figure 3 illustrates the definitions of interior and boundary. The pink region represents firm  $i$ ’s subgraph  $G_i$ , the green nodes are in the interior  $F_i$ , and the purple nodes are in the boundary  $G_i \setminus F_i$ .

Figure 3: Interior and Boundary



Next, let us define flares and islands in graph-theoretic terms.

**Definition 5** (Flares and Islands). A connected component  $L$  of the interior  $F_i$  of firm  $i$  is said to be an *island of firm  $i$*  if  $L$  is also a connected component of  $G$ , and said to be a *flare of firm  $i$* , otherwise.

For example, two flares and one island (the triangle on the right) exist in Figure 3. In the next subsection, we refine these notions using numerical indices. As defined above, a flare may not always “look like” what one may imagine to be a flare.

## 2.5 Measuring Flares

We introduce the following definition and proposition, which serve as the foundations for defining our concept of flare length.

**Definition 6** (Exit distance). Let  $u \in F_i$  be a node in the interior of firm  $i$ . The exit distance of  $u$  in  $F_i$  is

$$e_i(u) = \min\{d(u, w) \mid w \in G \setminus F_i\}.$$

In the case in which no path exists from  $u$  to any  $w \in G \setminus F_i$ , we put  $e_i(u) = \infty$ .

**Proposition 7.** *Let  $u \in F_i$ . Then,*

$$e_i(u) = \min\{d_{G_i}(u, v) \mid v \in G_i \setminus F_i\},$$

where  $d_{G_i}(u, v)$  is the distance between  $u$  and  $v$  in  $G_i$ .

See Appendix A for the proof. Using Proposition 7, we can compute  $e_i(u)$  using only the information of  $G_i$ , because the distance  $d_{G_i}(u, v)$  is the minimum length of all paths in  $G_i$  from  $u$  to  $v$ . By contrast, directly using Definition 6 would necessitate the computation of  $d(u, w)$ , the minimum length of all paths in  $G$  from  $u$  to  $w$ .

We use the exit distance  $e_i(u)$  to refine our notion of flares.

**Definition 8** (Flare index). For a connected component  $L$  of  $F_i$  (a flare or island of firm  $i$ ), the *flare index* of  $L$  is defined to be

$$k_i(L) = \max_{u \in L} e_i(u).$$

We immediately obtain the following characterization of islands using  $k_i$ .

**Lemma 9.** *Let  $L$  be a connected component of  $F_i$ . Then,  $k_i(L) = \infty$  if and only if  $L$  is an island of firm  $i$ .*

*Proof.* Immediate from the definitions. □

Finally, to aggregate all the information, we define flare signature.

**Definition 10** (Flare signature). Let  $F_i = L_1 \sqcup L_2 \sqcup \dots \sqcup L_M$  be a decomposition of  $F_i$  into its connected components. The *flare signature* of  $i$  is the multiset<sup>22</sup>

$$\vec{k}_i = \{\{k_i(L_j) \mid j = 1, \dots, M\}\}.$$

Note that if  $F_i$  is empty, we simply put the empty multiset as the flare signature of  $i$ .

We link the flare signature to the following “types.”

1.  **$\vec{k}_i$  is empty.** This case occurs if and only if  $F_i = \emptyset$ , meaning every node containing firm  $i$  neighbors at least one node not containing  $i$ . We call this case **Type 0: no flare or island**.
2.  **$\vec{k}_i$  contains only finite elements.** In this case, each connected component  $L$  of  $F_i$  is connected to some point  $w \in G \setminus F_i$ , meaning each  $L$  itself cannot be a connected component of  $G$ . Thus, each  $L$  is not an island; it is a flare. We call this case **Type 1: flares only**.
3.  **$\vec{k}_i$  contains finite elements, and some copies of  $\infty$ .** This case corresponds to **Type 2: flares and islands**.
4.  **$\vec{k}_i$  contains only copies of  $\infty$ .** This case corresponds to **Type 3: islands only**.

The flare signature is defined as a multiset of flare indices. Sometimes, having one number describing how much firm  $i$  looks like a flare in the Mapper graph may be convenient. Thus, we define the following.

**Definition 11** (Flare length). The *flare length* (or just *length*, for short) of firm  $i$  is

$$k_i = \begin{cases} 0 & \text{if } \vec{k}_i \text{ is empty,} \\ \text{finmax}(\vec{k}_i) & \text{if } \vec{k}_i \text{ has at least one finite element,} \\ \infty & \text{otherwise,} \end{cases}$$

where  $\text{finmax}(\vec{k}_i)$  is the maximum among all finite elements of  $\vec{k}_i$ .

Type 0 gets flare length 0, type 3 is sent to index  $\infty$ , and types 1 and 2 occupy the range in between, where the flare length of a firm is determined by the “longest” flare of firm  $i$ .

---

<sup>22</sup>A multiset is a modification of the concept of a set that, unlike a set, allows for multiple instances for each of its elements. We denote it by double braces  $\{\{, \}\}$  to distinguish it from a set.

**Computation of Flare Signatures** Let  $G = (V, E)$  be the Mapper graph of our data  $X$ . For each firm  $i$ , the computation of the subgraph  $G_i$  involving  $i$  can be done by iterating through all nodes  $v \in V$  and checking membership of firm  $i$  in  $v$ . The interior-boundary decomposition of  $G_i$  can be computed by considering the boundary first. For each  $v \in G_i$ , we simply check if  $v$  has a neighbor that is not in  $G_i$ ; if so,  $v$  is part of the boundary  $G_i \setminus F_i$ . The nodes of  $G_i$  not in the boundary are then automatically part of the interior.

Next, let us consider the computation of the flare signature  $\vec{k}_i$  of firm  $i$ . First, we need a decomposition of  $F_i$  into its connected components:

$$F_i = L_1 \sqcup L_2 \sqcup \dots \sqcup L_M,$$

which can be done, for example, via a breadth-first search. For each connected component  $L$  of  $F_i$ , its flare index is given by

$$k_i(L) = \max_{u \in L} e_i(u).$$

Because we need to do the same for each connected component  $L$  of  $F_i$ , we compute  $e_i(u)$  for all  $u \in F_i$ . By Proposition 7, the exit distance is

$$e_i(u) = \min\{d_{G_i}(u, v) \mid v \in G_i \setminus F_i\},$$

which can be computed using a multi-source version of Dijkstra’s shortest-path algorithm, with sources  $G_i \setminus F_i$ .

### 3 Data

**Patents** We use Ozcan’s (2015) data on patents that are granted by the USPTO between 1976 and 2010.<sup>23</sup> We use their application years (instead of years in which they are granted) in our analysis, because the former is closer than the latter to the time of actual invention. We focus on patents that are applied through 2005, because a substantial fraction of later applications would still be under review as of 2010, which raises concerns about sample selection. We sometimes call these patents “R&D patents” to distinguish them from “M&A

---

<sup>23</sup>Ozcan (2015) uses the USPTO’s Patent Data Files, which contain raw assignee names at the individual patent level. By contrast, the NBER Patent Data File (another commonly used source of patent data) records standardized assignee names at the “pdpas” (unique firm identifier) level, which is less granular than the original assignee name.

patents” (see below).

**Mergers and Acquisitions (M&As)** Aside from conducting in-house R&D and applying for patent protection, firms often obtain patents by acquiring firms that have their own portfolios of patents. Ozcan’s (2015) dataset links the USPTO data to the Securities Data Company’s M&A data module. This part of the dataset contains M&A deals between 1979 and 2010 in which both the acquiring firm and the target firm have at least one patent between 1976 and 2010.<sup>24</sup>

**Financial Performances** We use Compustat data on the firms’ revenues, EBIT (earnings before interest and taxes), and stock-market capitalization in 2005 (or the last available fiscal year if the firm disappears before 2005). Our purpose is to assess the relevance of our topological measures in terms of their correlations with the firms’ eventual financial performances (in section 5).

**Descriptive Statistics** To keep the sample size suitable for visual inspection and detailed exploratory analysis, we focus on firms that acquired at least four firms with patents between 1976 and 2005. This criterion keeps 333 major firms that conduct nontrivial amount of both R&D and M&A. Table 1 reports their descriptive statistics. The average patent count (2,081 for R&D and 268 for M&A) is much higher than the median, which suggests relatively few firms have disproportionately large portfolios even within our selective sample. The three financial-performance metrics exhibit similar skewness. Consequently, we use the natural logarithm of these variables to mitigate heteroskedasticity in our subsequent analysis (except for section 6, in which we use percentage shares).

**Where Do Firms Patent?** Panel (c) of Table 1 counts the number of USPTO classes in which the firms have patents. The median firm conducts R&D in 34.5 classes, whereas the mean is 65. The most diversified portfolio (Mitsubishi Electric) covers 358 of the 430 classes, followed by General Electric’s 347. Hence, the portfolio aspect of innovation is highly heterogeneous. Appendix A illustrates what these portfolios look like in raw data.

---

<sup>24</sup>The data include merger, acquisition, acquisition of majority interest, acquisition of assets, and acquisition of certain assets, but exclude incomplete deals, rumors, and repurchases. We use data on these transactions through 2005.

Table 1: Summary Statistics of 333 Major Firms

Variables	Number of observations	Mean	Median	Standard deviation	Minimum	Maximum
(a) Patent count						
In-house R&D	333	2,081	270	5,578	1	62,382
Acquired by M&A	333	268	59	883	4	9,453
Both R&D and M&A	333	2,349	405	5,833	5	62,561
(b) Financial performance						
Revenue (million US\$)	331	10,641	2,306	25,137	15	309,979
EBIT (million US\$)	331	1,429	250	3,763	-450	37,159
Market value (million US\$)	328	17,957	3,471	39,153	12	367,474
(c) Number of classes with > 0 patents						
In-house R&D	330	65.0	34.5	71.6	1	358
Acquired by M&A	326	22.5	12.5	30.4	1	225
Both R&D and M&A	333	72.4	43.0	72.3	2	358

*Note:* Financial-performance metrics are as of 2005 or the firm's last available fiscal year. Panels (b) and (c) display fewer observations than the sample size, because some firms are not in Compustat and some patents' classes are unknown.

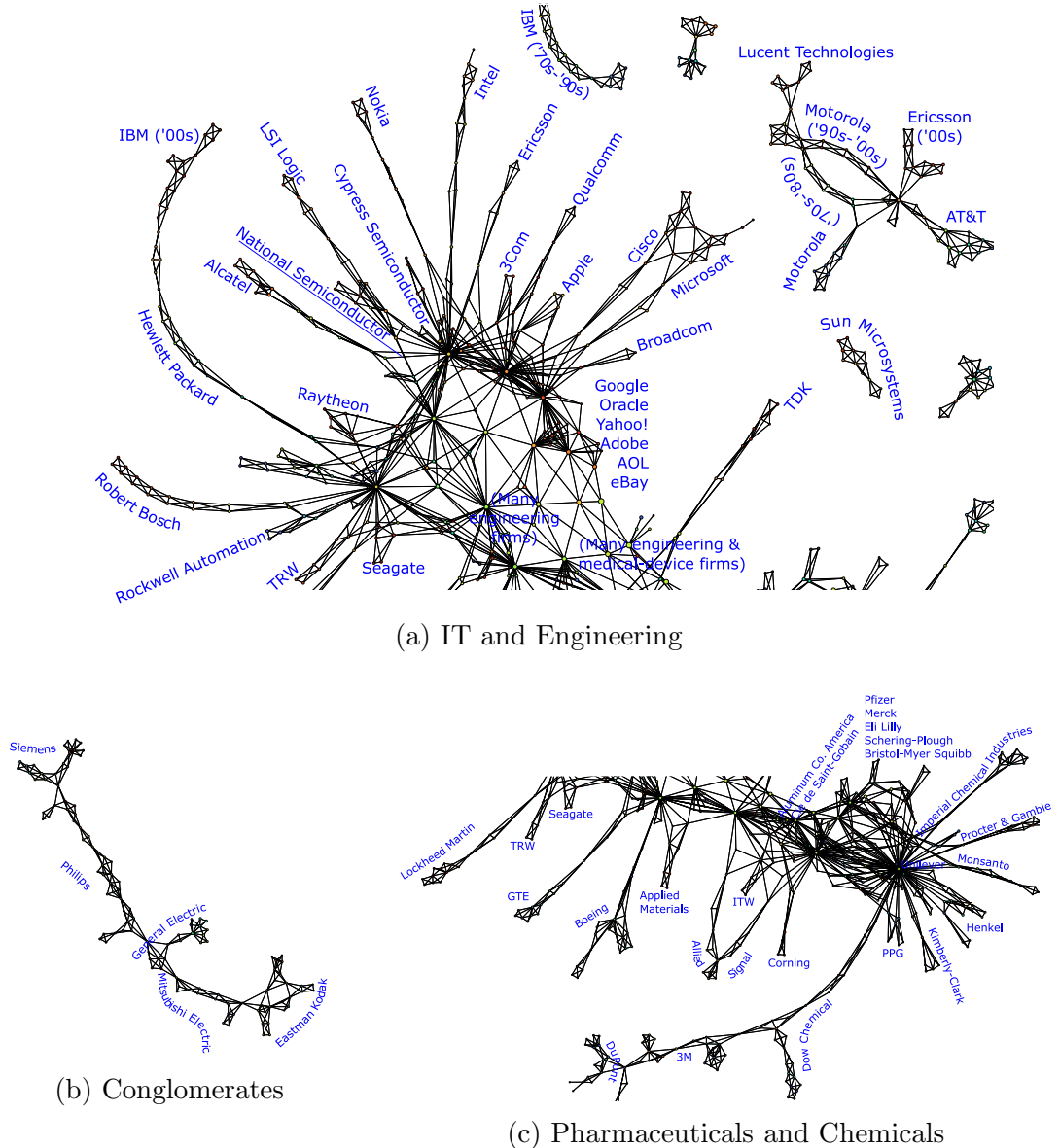
## 4 Mapping Patent Portfolios and Their Evolution

This section presents our first main result: visualization and description of technological space through our Mapper procedure in section 2.3. We reproduce Figure 1 (b) with greater detail in Figure 4 below and investigate its details. Unlike most other empirical studies in which data visualization plays a secondary role, this map embodies one of our main results, because mapping the high-dimensional space of technologies is the central empirical problem that this paper tackles.

**IT** Figure 4 (a) shows the northern half of Figure 1 (b). The main trunk consists of densely connected large nodes, each of which contains dozens of firm-years (e.g., the lower-middle part labeled “many engineering & medical-device firms”), because their portfolios are undifferentiated from each other.

Famous IT firms spike out from the trunk in flares, including Hewlett Packard (HP), Nokia, and Intel. They too start from the densely populated “heartland” of electronics and engineering in the 1970s. But their patenting behaviors diverge in the 1980s and evolve into something unique in the 1990s and the 2000s. This chronological pattern coincides with the underlying trend in which IT emerged as a major sector with technological opportunities in multiple different directions. According to the NBER patent database, computers and electronics relate to many USPTO classes: 35 classes (mostly in the 300s and the 700s) belong to “computers and communications” technologies, and 52 classes (mostly in the 300s

Figure 4: Mapper Graph (Details)



*Note:* Node colors represent the average year of the firm-years in that cluster, with earlier years in blue and later years in red. These figures are enlarged and more detailed versions of the Mapper graph of R&D patents in Figure 1, which uses log-transform, cosine distance,  $n = 20$ , and  $o = 0.5$ . See section 2.3 for details. Appendix Figure 9 shows another version with both R&D and M&A patents.

as well) belong to “electrical and electronic.”<sup>25</sup>

Some of the big names are extremely unique, thus forming their own “islands,” or smaller connected components that are isolated from the continent. For example, IBM had no peers

<sup>25</sup>By contrast, only 14 classes are categorized as “drugs and medical.” We discuss them in the following.

in the 1970s–1990s (see its small island in the upper-middle part). Its R&D activities were massive, diverse, and different from any other firm’s. Its restructuring in the early 2000s made it somewhat comparable to HP, as suggested by their rendezvous at the end of HP’s flare (see the top-left part).<sup>26</sup>

Other global brands display surprisingly short flares, for multiple reasons. Consumers might perceive Apple’s products as innovative, but their main appeal is design and functionality, which do not necessarily represent patentable inventions. Most software/internet firms (e.g., Google, Adobe, and eBay) were relatively new during the sample period and did not have time to develop unique patent portfolios.

Another curious case is Cisco and Microsoft, both of which heavily patented in classes 370 and 709 in the late 1990s.<sup>27</sup> Their substantial overlap connects the two flares in the middle, without which they would have looked separate and longer. This example highlights an important aspect of our analysis: uniqueness is a relative concept. That is, a firm’s flare length is determined by not only its own patenting patterns, but also all other firms’ trajectories, because it is based on the entire graph.

**Engineering Conglomerates** Famous engineering firms cluster together and constitute a large island in Figure 4 (b). General Electric (GE), an archetypical conglomerate, holds the most diversified portfolio in our data. Its only peers are similarly diversified manufacturers of electronic and capital goods, such as Siemens, Philips, and Mitsubishi Electric.

**Pharmaceuticals and Chemicals** Health care is another R&D-intensive sector, and patent protection is crucial for its business model. Unlike IT firms, however, pharmaceutical firms do not appear in flares. Large drug makers, such as Pfizer, Merck, and Eli Lilly, are clustered in the opposite side from IT firms, as Figure 4 (c) shows, because most of the drug patents are in either class 424 or 514 (both are labeled “drug, bio-affecting, and body-treating compositions”), which limits the extent to which their patent portfolios could differ from each other. Hence, further investigations into pharmaceutical innovation would require subclass-level data or a different data-transformation protocol (see section 6).

Household chemical brands appear near drug makers, usually in flares that grow outward, because their products are based on similar materials and technologies. Johnson and Johnson (J&J), Unilever, Procter and Gamble (P&G), and Kimberly-Clark hold patents in not only

---

<sup>26</sup>Flares reflect continuous changes over time. Sudden jumps, such as the disconnection within IBM between the 1990s and the 2000s, tend to occur when firms go through major corporate reorganization.

<sup>27</sup>USPTO class 370 is “multiplex communications” and class 709 is “electrical computers and digital processing systems: multicomputer data transferring.”

classes such as 510 (cleaning compositions for solid surfaces, auxiliary compositions therefor, or processes of preparing the compositions), but also 424 (see above) and 604 (surgery).

Monsanto, an agrochemical firm, appears in another flare that connects with drug makers. However, a closer look into its time path reveals the flare is moving *inward*, rather than outward as in the case of most other firms. Its patents in the 1970s and the 1980s are mostly unrelated to drugs, but those in the 1990s and the 2000s are in areas in which drug makers patent. Monsanto is one of the few centripetal flares in the graph, which suggests the firm employed highly idiosyncratic R&D strategies.

Finally, conglomerates in general chemistry (Dow, DuPont, and 3M) form their own long flares at the southern end of the continent. This pattern is reminiscent of the engineering conglomerates' island in Figure 4 (b). The ability to capture and visualize the relative proximity of conglomerates appears to be a unique strength of our approach, because their entire business portfolios are often too large and complicated to study otherwise (e.g., by using conventional IO methods at the individual product-market level).

**Patents Acquired by M&As** Figures 1 and 4 show the Mapper graph of R&D patents. How does the picture change if we incorporate M&A patents as well? Appendix Figure 9 shows another graph based on both R&D and M&A patents. The overall pattern looks familiar, because only 11.4% of all patents are obtained by M&As. Nevertheless, this addition alters the appearance of certain sectors. The main change is that more connections are formed. Computers, semiconductors, and telecommunications firms now form “super flares” that contain multiple firms in the same industries, respectively, rather than individually spiking out from the main trunk. Even IBM, whose patents in the 1970s–1990s form an island in the previous graph, is now part of the computer super flare. Likewise, whereas AT&T and other large telecommunications firms form their own island in Figures 1 and 4, this telecom island becomes a “peninsula” in Figure 9 and is connected to the main continent via Nokia’s flare. The manufacturers of semiconductor devices (e.g., Intel, Texas Instruments, and LSI Logic) form another super flare as well.

Aerospace and engineering firms go even further and form a “loop” instead of individual flares or super flares. That is, their extended (R&D + M&A) patent portfolios connect with the main trunk at multiple points. This pattern suggests these firms operate in a continuum of technological areas that relate to multiple different sectors.

Thus, even though M&A patents account for a small fraction of our sample, they do seem to materially expand the firms’ coverage areas. M&A patents seem to “fill in the gaps” between firms and make their eventual portfolios more similar to each other than the

R&D-only versions are. This tendency seems particularly strong in IT-related industries. By contrast, engineering conglomerates, pharmaceuticals, and chemical firms exhibit relatively small changes. They are already clustered together and densely connected in the previous graph; hence, M&A patents can add only so many connections.

## 5 Flares and Firms’ Performances

This section presents our second main result: the measurement of flare length and an exploration into its correlation with firms’ performances.

Even though not all flares can be recognized by visual inspection, the formal definitions and computational methods in sections 2.4 and 2.5 allow us to capture and characterize *all* firms’ flares, including those that are located within the densely populated areas. Table 2 shows the results. Whereas our visual inspection of Figure 4 in the previous section identified only a few dozen flares and islands, this systematic examination reveals the existence of many more. We find 40.3 % of our sample (133 firms) shows some flares.

Table 2: Firm Count by Flare Length

Flare length	0	1	2	3	4	5	6	7	8	$\infty$ (island)
Frequency	197	78	19	13	10	5	3	1	1	3
Percentage	59.70	23.64	5.76	3.94	3.03	1.52	0.91	0.30	0.30	0.91
Cumulative %	59.70	83.33	89.09	93.03	96.06	97.58	98.48	98.79	99.09	100.00

*Note:* The underlying Mapper graph uses log-transform, cosine distance,  $n = 20$ , and  $o = 0.5$ . See section 2.3.

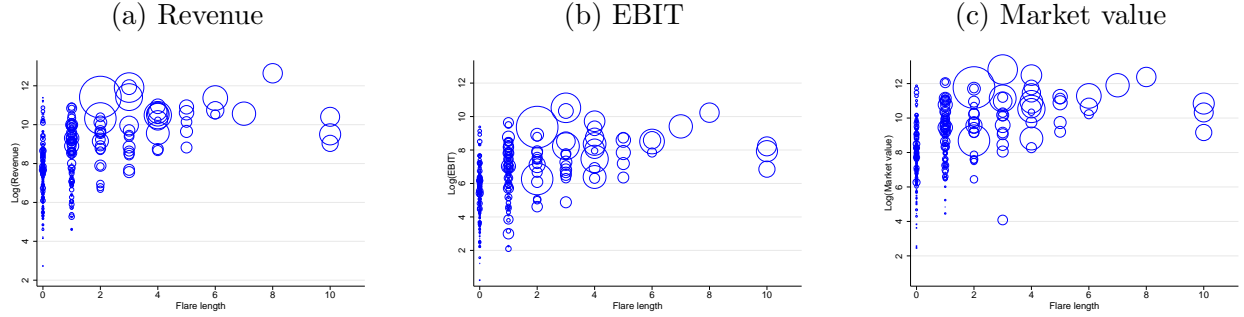
**What Makes Portfolios “Unique”?** Raw data at the firm level, such as those reviewed in Appendix A, suggest both the quantity and variety of patents help make their portfolios unique. For example, HP has a massive portfolio and has a flare of length 6, whereas Dell’s portfolio is much smaller and its flare length is 1.<sup>28</sup> However, these conditions are not sufficient for long flares, because uniqueness is a relative concept. Our definition of flare length is based on *the graph of all firms in all years* and their distances from each other. Hence, our notion of *technological differentiation* shares the spirit of product differentiation

<sup>28</sup>Note HP and Dell are among the largest computer makers, and their main patent classes are similar, but their approaches to R&D are different. HP is a traditional computer maker, whereas Dell’s success is usually attributed to its unique business model in which the company sells directly to consumers and most of the manufacturing is outsourced to third-party suppliers in Asia. Such “business-model innovations” do not represent patentable inventions in most cases. Hence, patent statistics (and their topological representations) do not reflect Dell’s “uniqueness” in this sense.

in standard IO models, and the firm’s flare length depends on not only its own activities but also all other firms’.<sup>29</sup>

In the remainder of this section, we investigate whether flares contain any “relevant” information. Following a common practice in the patent statistics literature (e.g., Pakes and Griliches (1984), Jaffe (1989), and Hall, Jaffe, and Trajtenberg (2005)), we look for correlations between these topological characteristics and the firms’ performance metrics, including revenue, profit, and stock market value.

Figure 5: Flares and Financial Performances



*Note:* The center of each circle represents the firm’s revenue in 2005 (on the vertical axis) against the flare length of its patents in 1976–2005 (on the horizontal axis). The circle size reflects the firm’s total patent count across all classes and all years. Infinitely long flares (i.e., islands-only type) are shown at length 10 for illustration purposes.

**Scatter Plots** Figure 5 (a) plots each firm’s revenue in 2005 (on the vertical axis) against the flare length of its patents in 1976–2005 (on the horizontal axis). The circle size reflects the total count of patents in 1976–2005. The maximum finite flare length of all firms is 8; the figure shows infinitely long flares (i.e., islands-only type) at length 10 for ease of visualization. Two patterns emerge. First, the upper-triangle-like shape of the scatter plot suggests long flares always entail high revenues, but the reverse is not true. Some high-revenue firms show short or no flares. Second, the prevalence of large circles in the upper region suggests large portfolios are frequently associated with both high revenues and long flares. However, some firms have many patents but only short flares of length 2 or 3. Thus, long flares predict high revenues and many patents, but not all “large” firms exhibit long flares. Panels (b) and (c) show similar patterns for profit and market value, respectively.

<sup>29</sup>Qualcomm, a manufacturer of telecommunication chips, exemplifies this point with a unique portfolio (length 3) despite having relatively few patents and seemingly simple distribution across classes. See Appendix Figures 11 and 12 for a comparison of HP, Dell, and Qualcomm.

These patterns are not an artifact of aggregation or driven by a few specific sectors and industries. Appendix Figure 10 plots revenues and flares by economic sector defined by Standard and Poor's (S&P), a credit-rating agency. Appendix Figure 11 studies the technology sector more deeply at the SIC-code level, with a focus on computers and semiconductor industries. These additional scatter plots show the positive correlations are preserved within each sector and industry.

**Regressions** Let us further investigate these correlations by running regressions of the following form:

$$\ln(y_i) = \alpha_1 + \alpha_2 k_i + \alpha_3 \mathbb{I}\{k_i = \infty\} + \alpha_4 \ln(p_i) + \varepsilon_i, \quad (5)$$

where  $y_i$  is firm  $i$ 's revenue (or other performance metrics) in 2005,  $k_i$  is the flare length of its patent portfolio's evolution in 1976–2005,  $\mathbb{I}\{k_i = \infty\}$  is a dummy variable indicating the islands-only type,  $p_i$  is the total count of firm  $i$ 's patents in 1976–2005 (i.e.,  $p_i = \sum_t \sum_c p_{i,t,c}$ ),  $\alpha$ s are their coefficients, and  $\varepsilon_i$  is an error term.<sup>30</sup> We include  $\ln(p_i)$  to control for the size of the firm's R&D/patenting activities.

Table 3: Flares, Counts, and Performances

LHS variable:	Log(Revenue)			Log(EBIT)			Log(Market value)		
	(1)	(2)	(3)	(4)	(5)	(6)	(7)	(8)	(9)
Constant (= no flare)	7.38 (0.10)	5.65 (0.20)	6.08 (0.22)	5.35 (0.10)	3.56 (0.22)	3.97 (0.24)	7.80 (0.10)	5.86 (0.22)	6.20 (0.24)
Flare length	0.65 (0.06)	— (—)	0.34 (0.08)	0.65 (0.07)	— (—)	0.33 (0.08)	0.66 (0.07)	— (—)	0.27 (0.08)
Islands only	2.27 (0.86)	— (—)	0.95 (0.84)	2.32 (0.91)	— (—)	0.94 (0.88)	2.31 (0.94)	— (—)	0.70 (0.90)
Log(Patents)	— (—)	0.40 (0.03)	0.28 (0.04)	— (—)	0.41 (0.04)	0.29 (0.05)	— (—)	0.44 (0.04)	0.34 (0.05)
$R^2$	.261	.305	.345	.256	.308	.345	.233	.320	.343
Adjusted $R^2$	.257	.303	.339	.251	.306	.338	.228	.317	.336
Number of observations	328	328	328	301	301	301	325	325	325

*Note:* The LHS variables are as of 2005 or the latest years available in Compustat. The RHS variables are based on our topological characterization (via cosine distance) of the patent statistics in 1976–2005. The number of observations varies across columns, because some firms in our patent database lack information on certain performance metrics in Compustat. In columns 4–6, firms with negative EBIT drop out due to log-transformation. See Appendix Table 6 for results based on other distance metrics, and Tables 7 and 8 for results based on balanced panels. Standard errors are in parentheses.

Table 3 shows flare length is positively correlated with the firm's revenue, EBIT, and

<sup>30</sup>Note we do not intend to prove causal relationships. Our purpose is to assess the extent to which our uniqueness measures predict these performance metrics.

market value in 2005. Columns 1, 4, and 7 use the flare variables alone; columns 2, 5, and 8 use  $\ln(p_i)$  alone; and columns 3, 6, and 9 use both. The purpose of comparison is to assess whether our topological characteristics convey additional information above and beyond what patent count alone could predict. The differences between the adjusted  $R^2$ s suggest they do. More formally, the F-tests of a linear restriction,  $\alpha_2 = \alpha_3 = 0$ , reject the null hypothesis at the 0.01%, 0.1%, and 1% levels for the revenue, EBIT, and market-value regressions, respectively.<sup>31</sup> Hence, the incremental contribution of the flare-and-island variables is statistically highly significant.

What about their economic significance? The estimates of  $\alpha_2$  are 0.34, 0.33, and 0.27 in columns 3, 6, and 9 (i.e., after controlling for  $p_i$ ), respectively, which imply an extra length of flare is associated with 40%, 39%, and 31% higher performances in terms of revenue, EBIT, and market value, respectively.<sup>32</sup>

**Robustness to Alternative Distance Metrics and Survivorship Bias** These findings are robust to both the choice of distance metrics and firm survivorship (i.e., the possibility that both flare length and the eventual financial performances might be driven by a third factor: the duration of firm survival). Appendix Table 6 shows the results are similar under alternative distance metrics that are commonly used in the literature. Appendix Tables 7 and 8 show the same patterns hold in balanced panels.

**Why Do Flares Correlate with Performances?** Why do successful firms grow long flares? Or, why do flares reflect the firms' success and failure? Three factors would seem to constitute the underlying mechanism: size, growth, and market power.

First, larger firms tend to spend more on R&D and obtain more patents. This pattern is well documented in the innovation literature (Cohen, 2010). To the extent that high  $p_i$  allows the firm to exhibit more uniqueness (i.e., a higher degree of freedom in shaping the distribution of patents across different classes), having a certain size might be a necessary condition for unique portfolios. However, our regressions control for  $p_i$  in columns 3, 6, and

---

<sup>31</sup>We calculate  $F = [(R_{ur}^2 - R_r^2)/2]/[(1 - R_{ur}^2)/(\#obs - 4)]$ , where  $R_{ur}^2$  is the  $R^2$  of the unrestricted model in column 3 (6 or 9),  $R_r^2$  is the  $R^2$  of the restricted model in column 2 (5 or 8), and  $\#obs$  is the number of observations (328, 301, or 325). We reject the null hypothesis,  $\alpha_2 = \alpha_3 = 0$ , if  $F$  is greater than the corresponding critical value of the F distribution.

<sup>32</sup>Likewise, the estimates of  $\alpha_3$  (0.95, 0.94, and 0.70 in the same three columns) suggest islands-only firms tend to outperform no-flare firms by 159%, 156%, and 101% in these measures, respectively. However, their standard errors are large. Only a few firms belong to this category, and all of them have relatively large patent portfolios, which makes  $\alpha_3$  difficult to isolate from  $\alpha_4$ . Nevertheless, we keep  $1\{k_i = \infty\}$  in these columns, because dropping it (and thereby grouping them with no-flare firms) would be unwise in light of Figure 5 and other results (columns 1, 4, and 7).

9. Moreover, a “large but stagnant” portfolio would not exhibit long flares, because  $p_{i,t}$  and  $p_{i,t+1}$  (say) would remain identical and cluster together in that case. Hence, *size* alone cannot explain the results; for a firm to develop flares, its portfolio must also be *growing* and *differentiated*.

The second factor is growth. If the firm stops expanding its R&D activities, its evolution on the Mapper graph would also stop. Other abrupt changes, such as corporate restructuring (e.g., scaling down or refocusing R&D efforts), could also hamper the steady growth of long flares. Even though anecdotal success stories of “corporate turnaround as a result of radical transformation” exist, the positive correlations in Table 3 suggest such cases are rare, at least in our data. Hence, long flares could be symptomatic of sustained growth.

We already discussed the third factor, differentiation, at the end of section 4. Its connection to financial performances is straightforward, as almost any model of imperfect competition can explain how product differentiation softens price competition and increase profits. To the extent that successful product differentiation relies on technological differentiation, unique R&D and patents could predict (or at least proxy for) subsequent competitive advantage and market power.<sup>33</sup>

## 6 Comparison with Jaffe (1989)

This section presents our third main result: an alternative map of technological space based on Jaffe’s (1989) data-transformation convention, as well as a comparison of this map with his clustering method.

How does our approach compare with Jaffe’s (1989) clustering method? Both use the same type of data in which a firm-year is represented by a vector of patent counts, and seek to map firms’ locations in the technological space. Table 4 clarifies two differences.

First, we take a logarithm of patent count,  $x_{i,t,c} = \ln(p_{i,t,c} + 1)$ , whereas he takes a share of each class within a firm-year,  $x_{i,t,c} = \frac{p_{i,t,c}}{\sum_c p_{i,t,c}}$ . These rescaling protocols transform the metric space itself and lead to significant differences in the outputs. Hence, how one pre-processes raw data is an important, substantive choice. Nevertheless, this difference is secondary in terms of methodology, because it is a matter of data pre-processing rather than the analytical procedure itself. As we demonstrate in this section, we can easily switch to Jaffe’s share-based measure while sticking to our overall framework.<sup>34</sup>

---

<sup>33</sup>Building a micro-founded model that incorporates these mechanisms (and implementing it empirically) is beyond the scope of this paper. We leave the task for future research.

<sup>34</sup>Likewise, one can use our logged patent counts within Jaffe-style clustering.

Table 4: Comparison with Jaffe (1989)

Procedures	Ours (sections 1–5)	Ours (this section)	Jaffe (1989)
1. Re-scaling	Log	Share	Share
2. Distance metric	Cosine	Cosine	Cosine
3. Clustering	Local	Local	Global
4. Reconstruction	Edges	Edges	None
5. Final output	Graph	Graph	Clusters

*Note:* We may use other distance metrics in the Mapper procedures, including Euclidean, correlation, min-complement, and Mahalanobis. See various sensitivity analyses in the Appendix.

The second and more important difference is that Jaffe performs clustering at the global level to generate a list of mutually exclusive clusters of firms, whereas our “clusters” are local and retain connections through edges between them (which reflect the existence of commonly shared members). In other words, his algorithm is a big *discretization* operation, whereas ours is designed to recover the *continuum* of firms and industries in the data. Uncovering the original, continuous data patterns is important because industry boundaries could be fluid especially when innovative activities are concerned. In the following, we demonstrate how our method can help reveal the global shape of the data and generate additional insights beyond what Jaffe-style clustering does.

As a point of departure, Table 5 shows a list of clusters that global clustering à la Jaffe generates. The grouping seems intuitive, with clusters of firms in engineering (cluster 1), telecommunications (cluster 2), materials (cluster 3), medical devices (cluster 4), pharmaceuticals (cluster 5), and so on. However, cluster boundaries are ultimately an artifact of discretization. Some firms belong to multiple clusters over the years, and hence would appear to “move” between technological fields. Jaffe (1989) investigates such “movers” in detail. The reality, however, is that cluster boundaries are frequently drawn in the middle of their data points (firm-years), and not necessarily that they moved a lot in the original technological space.

The flip side of this boundary issue is that some industries and technologies are intrinsically connected and form a continuum. Splitting them into separate groups would be unnatural in such cases. For example, clusters 7 (computers), 10 (semiconductors), and 11 (electronics) commonly share Intel and HP as their group members. One interpretation is that these firms are exceptionally active in many different fields, but another is that these industries and technologies form a continuum, founded upon closely related (electrical and electronic engineering) methods, and should not be treated separately. Likewise, one might

Table 5: K-Medoids Clustering à la Jaffe (1989)

Cluster	Number of firm-years	Number of unique firms	Representative firms (non-exclusive list of longest-appearing firms in each cluster)
1	814	88	Bosch, Halliburton, Schlumberger, Westinghouse
2	576	57	Ericsson, Alcatel, AT&T, Siemens, Qualcomm
3	548	61	Saint-Gobain, 3M, International Paper, TDK, Alcoa
4	461	35	Stryker, Kimberly-Clark, C.R.Bard, Baxter Travenol, J&J, P&G
5	433	37	Abbott, Eli Lilly, Merck, Pfizer, Sandoz, Schering-Plough
6	371	40	Dow, DuPont, Henkel, Bayer, Monsanto, Bausch & Lomb
7	365	56	Seagate, Unisys, IBM, Dell, Sun, Intel, HP
8	303	38	Millipore, Pall, Parker Hannifin, Osmonics, Dover, U.S.Filter
9	287	38	Lockheed Martin, Raytheon, BAE Systems, Northrop Grumman
10	285	23	TI, National Semiconductor, LSI Logic, Cypress, Intel, Motorola
11	283	44	Tektronix, Teradyne, Philips, Varian, HP, Baker Hughes
12	262	41	Pitney Bowes, BMC Software, Oracle, AOL, Yahoo!, Google, eBay
13	237	31	Asyst, Rubbermaid, K2, Tenneco Automotive, TRW
14	234	27	Teleflex, Eaton, Dana, Deere, EG&G, Roper Industries
15	214	31	Chiron, Amgen, Genzyme, Invitrogen, Beckman Coulter, Monsanto
16	195	27	Apple, Silicon Graphics, Adobe, Sun, Dassault, Disney, NVIDIA
17	156	22	Coherent, Electro Scientific, Finisar, Newport, Corning, Alcoa, TRW
18	148	27	AMAT, Nordson, Advanced Energy, EMCORE, Cookson
19	141	14	Mattel, Hasbro, Leggett & Platt, Tyco, International Game Tech
20	73	9	Medtronic, Greatbatch, Cordis, Respiromics, Roper Industries
21	48	10	Nuance Communications, Lernout & Hauspie Speech, ScanSoft
Total	6,434	756	

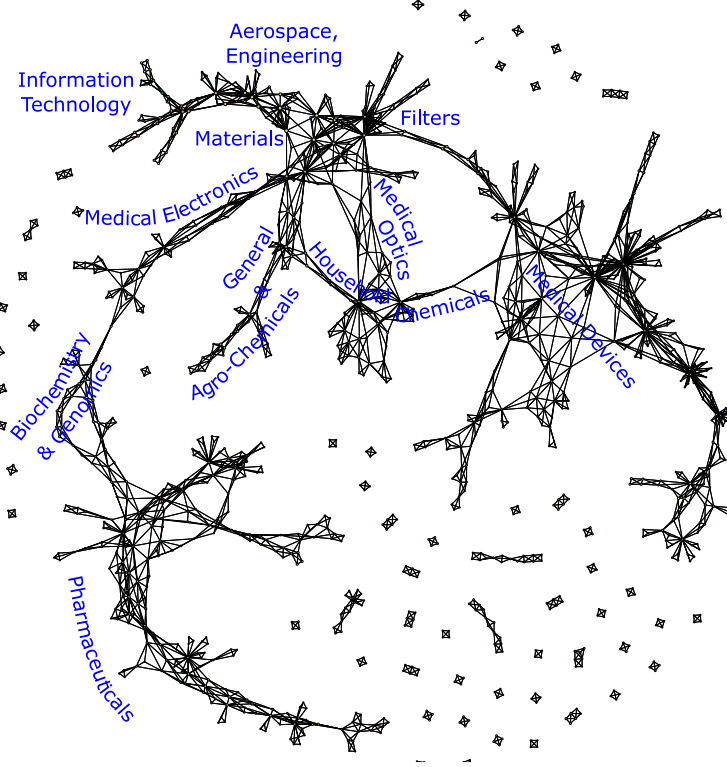
*Note:* The number of clusters (21) follows Jaffe's original specification. The total number of unique firms exceeds 333, because many firms appear in multiple clusters. Whereas Jaffe (1989) uses k-means clustering, we use its variant, k-medoids clustering. K-means clustering of our data leads to an extreme result in which a single cluster contains more than 70% of all firm-years, because so many firm-years are located in the densely populated neighborhood of electronics and engineering (i.e., the upper north region of Figure 6). See Appendix Table 9 for the result of k-means clustering à la Jaffe (1989).

question whether Monsanto is particularly mercurial in moving between clusters 6 (chemicals) and 15 (genomics), or if they are simply two faces of the same, connected discipline. Yet another example is medical-device manufacturers, which are somehow split into two clusters (4 and 20). Many of these results could be an artifact of discretization.

Our approach preserves the underlying continuity in the data. Figure 6 is the Mapper graph of the same data, based on the same rescaling protocol (percentage shares) and the same distance metric (cosine). Unlike the 21 mutually exclusive groups from the global clustering method, the shape graph recovers a *continuum of industries* from the data. Indeed, its main insight is that industries are connected, sometimes in unanticipated ways. We examine some of the most conspicuous patterns in Figure 6 in the following.

**“Shrinking” High-Tech Industries** Many firms populate the upper-north-west corner of the graph. This high-tech region is so densely populated that disentangling it is difficult (see

Figure 6: Mapper Graph Based on Jaffe’s Measure



*Note:* Node colors represent the average year of the firm-years in that cluster, with earlier years in blue and later years in red. This figure is a shape-graph representation of 333 major firms' R&D patents in 1976–2005 based on shares, cosine distance,  $n = 40$ , and  $o = 0.5$ . See Appendix Figure 13 for a detailed version.

Appendix Figure 13, panel a). These firms conduct R&D in relatively many patent classes. Raw patent counts (and their logged version in sections 1–5) preserve the uniqueness of each firm’s portfolio. However, after their conversion into percentage shares (and hence the loss of information on volumes in absolute terms), most portfolios end up looking alike. Thus, the non-share-based Mapper graphs of sections 1–5 seem more informative about high-tech industries.

**Biomedical Super Flare** By contrast, the share-based Mapper graph maps biomedical areas more clearly and reveals interesting technological connections between industries.<sup>35</sup> Pharmaceutical companies live in their own world (in the south-west corner of Figure 6), patenting only in a few drug-related classes. Nevertheless, they are not completely isolated, because biochemistry and medical electronics firms stretch from the northern “heartland” of engineering, materials, and general chemicals. The detailed maps in Appendix Figure 13

<sup>35</sup>We thank Elizabeth Lyons for helpful discussions on these industries.

(panels a and b) show medical-equipment manufacturers (e.g., Perkin Elmer and Beckman Coulter) and genomics-based drug developers (e.g., Amgen and Genzyme) connect with pharmaceutical companies (e.g., Merck and Pfizer), collectively forming a long “archipelago” of biomedical industries. These connections are intuitive because genomics firms rely on measurement and data processing to develop new drugs. Uncovering them from Table 5 alone would be difficult because it classifies general and agro-chemicals in cluster 6 and biochemicals and medical electronics in cluster 15.<sup>36</sup>

**Two Bridges to Medical Devices** Medical-device manufacturers occupy a large territory in the eastern half of Figure 6.<sup>37</sup> The Mapper graph reveals somewhat surprising ways in which this industry connects with others. Specifically, two types of firms bridge between medical devices and the engineering heartland.

One bridge consists of household chemicals and contact lenses. Appendix Figure 13 (panels a and c) shows household names, such as Unilever, P&G, and Bausch & Lomb, were close to the center of materials and general chemicals in the 1970s and the 1980s. But then their R&D efforts moved in the south-east direction to form their own peninsulas by the 1990s and the 2000s. J&J has a major health care division and bridges between household chemicals and medical devices.

The other bridge is located in the north and builds on dense clusters of less well-known firms specializing in aerodynamics and filters (e.g., Sealed Air, U.S. Filter, and Mine Safety Appliance). It then extends in the south-east direction and connects with more obviously medical-device-related names, such as Respiration and Vital Signs. The two groups of firms are seemingly unrelated at first glance, but their underlying technologies are common: breathing requires clean air, and the monitoring of vital signs concerns fluid dynamics. Thus, technologically speaking, mine safety and medical devices are closer neighbors than what a conventional industry-classification system would suggest. By contrast, the global clustering in Table 5 is not particularly informative about these connections: P&G and J&J appear in cluster 4; the aerodynamics-and-filters firms appear separately in cluster 8; and medical devices are split into clusters 4 and 20.

---

<sup>36</sup>Both clusters prominently feature Monsanto as a member, but its unique trajectory does not conform to the patterns of any other firms in either cluster (except Bayer, which acquired it in 2018). Appendix Figure 13 shows Bayer did not move much throughout the sample period, whereas Monsanto made a long trip from the crowded center of materials and chemicals industries to Bayer’s location. The fact that Bayer acquired Monsanto in 2018 might suggest patent portfolios are a useful predictor of competitive positions and mergers. See European Commission (2017).

<sup>37</sup>We thank Matthew Grennan for helpful discussions on medical devices.

These examples highlight Mapper’s ability to preserve and represent the continuous patterns in the original space, which could help us draw many additional insights from otherwise intractable, high-dimensional data. Whereas Jaffe-style clustering generates a list of discrete, disjoint groups of firms (or firm-years), the shape graphs from Mapper put them in the global context and reveal continuity. Clustering has the beauty of simplicity; Mapper shows more nuances and the “big picture” at the same time. Thus, our approach is highly complementary to the existing methods and is a valuable addition to the toolbox for economists studying any *intrinsically high-dimensional* objects.

## 7 Conclusion

This paper proposes a new method to map, describe, and characterize firms’ inventive activities. The shape graphs from the Mapper procedure help us understand where firms and industries are located, how they connect with each other (or not), and how their innovative activities evolve over time. In the past, economists’ ability to answer these basic, descriptive questions—and hence the ability to ask and answer deeper, causal/policy questions *that presuppose reliable descriptions or stylized facts*—have been constrained by the “curse of dimensionality” of the technological space. With the new tool, we can start revisiting and answering some of the long-standing questions in economics, including the rate and direction of inventive activity. Because its underlying mathematics is general, we believe this method is potentially useful for describing and characterizing other high-dimensional data in economics as well, such as product characteristics and international trade.

## Appendix (For Online Publication)

### A. Raw Data: Where Do Firms Patent?

Let us illustrate with examples what the firms' patent portfolios look like. Figure 7 visualizes the evolution of patenting activities at six major firms. Each plot lists the 430 USPTO patent classes on the vertical axis, and the year of application (for R&D patents) or acquisition (for M&A patents) on the horizontal axis. The circle size represents the number of patents in each class-year.

The top panels show two IT firms. Cisco Systems makes network equipment (e.g., routers) and is famous for its active use of M&As to acquire new products and talents; it acquired the largest number of target firms with patents in our sample. Nevertheless, most of Cisco's patents are obtained by in-house R&D and are concentrated in classes 370 (multiplex communications) and 709 (electrical computers and digital processing systems: multicomputer data transferring). Seagate Technology makes hard disk drives (HDDs) and is another example of specialized IT firms. Its main patent class is 360 (dynamic magnetic information storage or retrieval), which is central to the HDD technology, but its portfolio gradually diversified as the firm intensified efforts to manufacture key components as well, including heads, media, and their interface.<sup>38</sup>

The middle panels show two health care firms. The pharmaceutical industry is R&D-intensive, but the patent portfolio of Pfizer looks simpler than the IT examples. Most of the drug patents are in classes 424 and 514 (drug, bio-affecting, and body treating compositions), and drug makers hardly patent elsewhere. By contrast, medical devices rely on a variety of technologies, even though their main classes are relatively few (600–607). The plot shows Medtronic, a leading medical-device maker, is active in many areas.

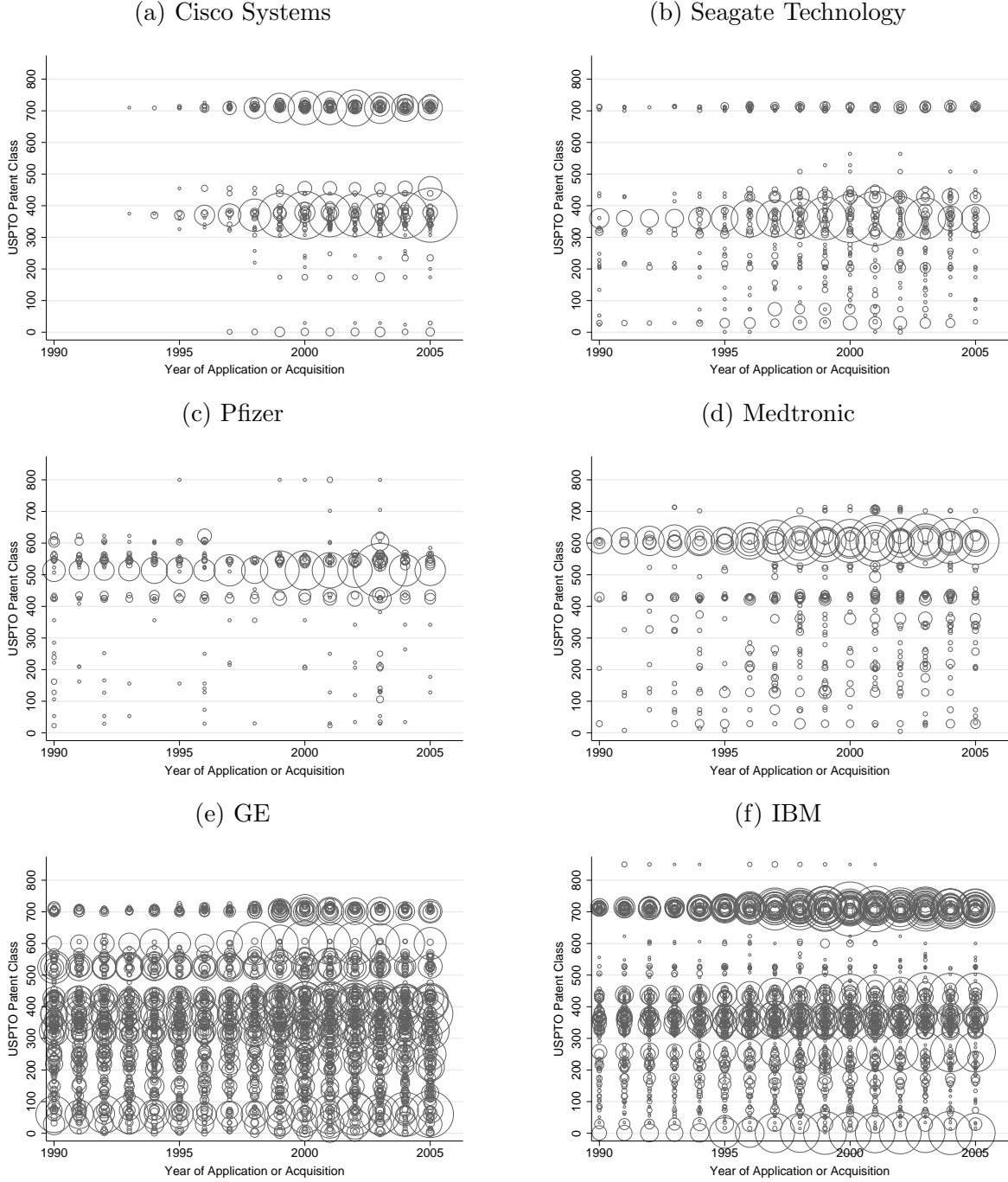
The bottom panels present extreme cases, for a reference. GE, a conglomerate, has one of the most diversified portfolios in our sample, with patents in more than 300 classes. The picture becomes too messy for human eyes to draw insights. Finally, IBM has by far the largest number of patents in our sample, but its portfolio looks more organized than GE's, because its activities are more focused. Most of the computers and electronics technologies are in the 300s and the early 700s, which are where IBM's portfolio is concentrated.

These examples suggest the portfolio aspect of patents and technologies is interesting and contains potentially important information. However, the high dimensionality of technological space makes conventional data analysis difficult.

---

<sup>38</sup>See Igami and Subrahmanyam (2019) for the details of patents and innovation in the HDD industry.

Figure 7: Acquiring a String of Pearls



*Note:* The circle size represents the number of patents in each class-year. Based on our method and analysis in sections 3 and 4, the “flare lengths” (our proposed measure of “uniqueness”) of these firms’ portfolios are: 3 (Cisco), 2 (Seagate), 1 (Pfizer), 2 (Medtronic), 4 (GE), and  $\infty$  (IBM).

## B. Proofs

First, we show the boundary  $G_i \setminus F_i$  indeed serves as a “boundary” for  $F_i$ : to get outside of  $G_i$ , one always needs to go through the boundary.

**Lemma 12.** *Let  $u \in F_i$  and  $w \in G \setminus G_i$ , and let  $p$  be a path from  $u$  to  $w$ . Then, the path  $p$  passes through some node  $v \in G_i \setminus F_i$ .*

*Proof.* Let  $p$  be such a path from  $u \in F_i$  to  $w \in G \setminus G_i$ , which passes through the nodes

$$u = v_0, v_1, v_2, \dots, v_{n-1}, v_n = w$$

in that order.

Suppose, to the contrary, that all  $v_j$  are not in the boundary  $G_i \setminus F_i$ . We show by induction that  $v_j \in F_i$  for all  $j \in \{0, \dots, n\}$ . First,  $v_0 = u \in F_i$  is clear. Suppose  $v_j \in F_i$ . Because  $v_{j+1} \in B_1(v_j) \subseteq G_i$  by definition of the interior  $F_i$ , and because  $v_{j+1} \notin G_i \setminus F_i$  by assumption, we see  $v_{j+1} \in F_i$ . Thus, by induction,  $v_j \in F_i$  for all  $j \in \{0, \dots, n\}$ . In particular,  $v_n = w \in F_i$ , which is a contradiction, because  $w \in G \setminus G_i \subseteq G \setminus F_i$ .

Therefore, some  $v_j$  exists in the boundary  $G_i \setminus F_i$ .  $\square$

For  $i$ , a firm, and  $u \in F_i$ , recall the exit distance of  $u$  in  $F_i$  was defined to be

$$e_i(u) = \min\{d(u, w) \mid w \in G \setminus F_i\}$$

in Definition 6. Here, we reproduce Proposition 7 and provide a proof.

**Proposition 13.** *Let  $u \in F_i$ . Then,*

$$e_i(u) = \min\{d_{G_i}(u, v) \mid v \in G_i \setminus F_i\},$$

where  $d_{G_i}(u, v)$  is the distance between  $u$  and  $v$  in  $G_i$ .

*Proof.* It is clear that

$$\min\{d(u, w) \mid w \in G \setminus F_i\} \leq \min\{d_{G_i}(u, v) \mid v \in G_i \setminus F_i\}.$$

Suppose the minimum of the left-hand side is achieved by a  $w \in G \setminus F_i$ , and let  $d(u, w) = \ell(p)$ , the length of a minimum path  $p$  in  $G$  from  $u \in F_i$  to  $w \in G \setminus F_i$ . Let  $v$  be the first node  $v \in G_i \setminus F_i$  that  $p$  passes through. Note such  $v$  exists by Lemma 12.

In the case in which  $v \neq w$ , truncate  $p$  to the path  $p'$  from  $u$  to  $v$ . By choice of  $v$ ,  $p'$  is fully contained in  $G_i$ , and  $\ell(p') < \ell(p)$  because we only have positive weights and  $p'$  has strictly fewer edges than  $p$ . It follows that

$$\min\{d(u, w) \mid w \in G \setminus F_i\} = \ell(p) > \ell(p') \geq \min\{d_{G_i}(u, v) \mid v \in G_i \setminus F_i\},$$

because  $p'$  is a path from  $u$  to  $v$  that is contained in  $G_i$ . This is a contradiction.

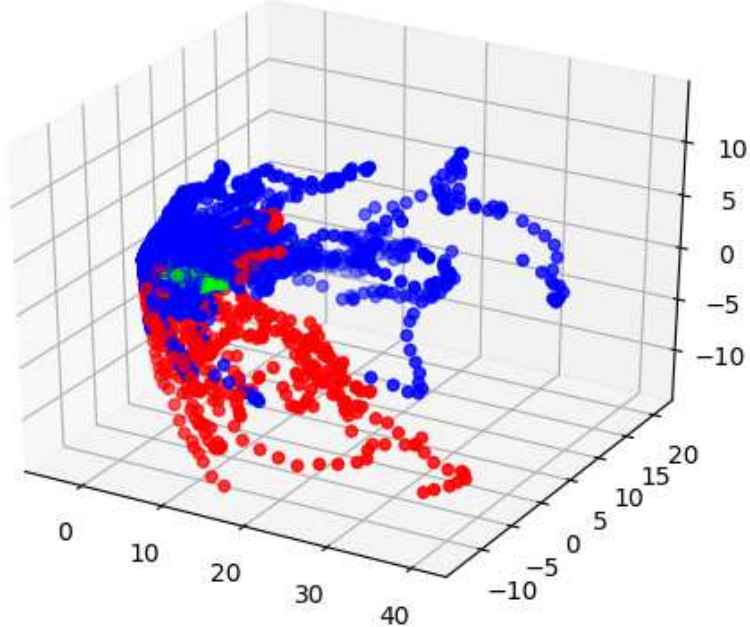
Thus,  $v = w$ , and it follows that

$$\min\{d(u, w) \mid w \in G \setminus F_i\} = \ell(p) \geq \min\{d_{G_i}(u, v) \mid v \in G_i \setminus F_i\},$$

which shows the required equality.  $\square$

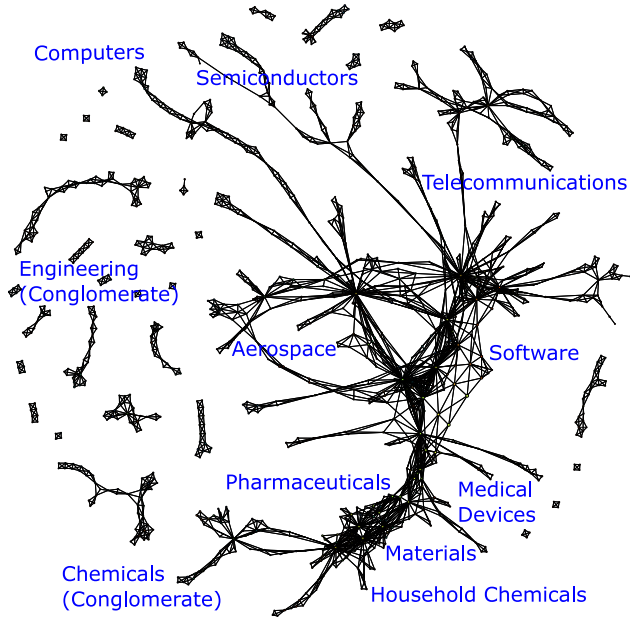
### C. Additional Figures and Tables for Sections 4, 5, and 6

Figure 8: Three-Dimensional PCA



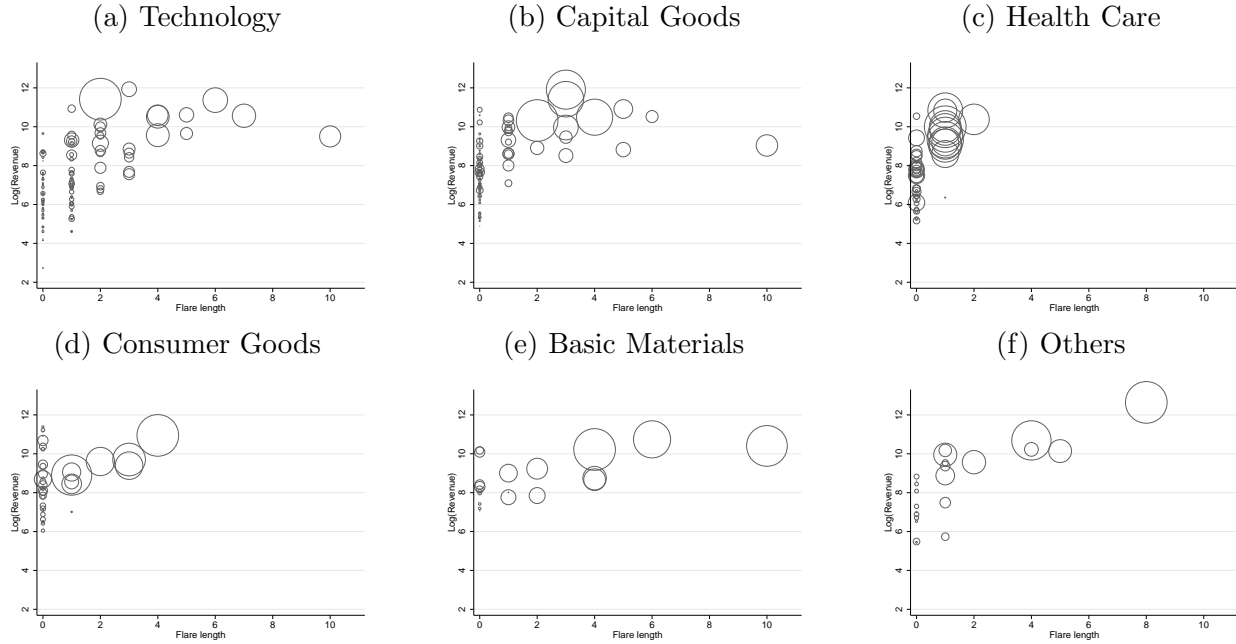
*Note:* Red markers are IT firms, green markers are drug makers, and blue markers are all others.

Figure 9: Mapper Graph of Both R&D and M&A Patents



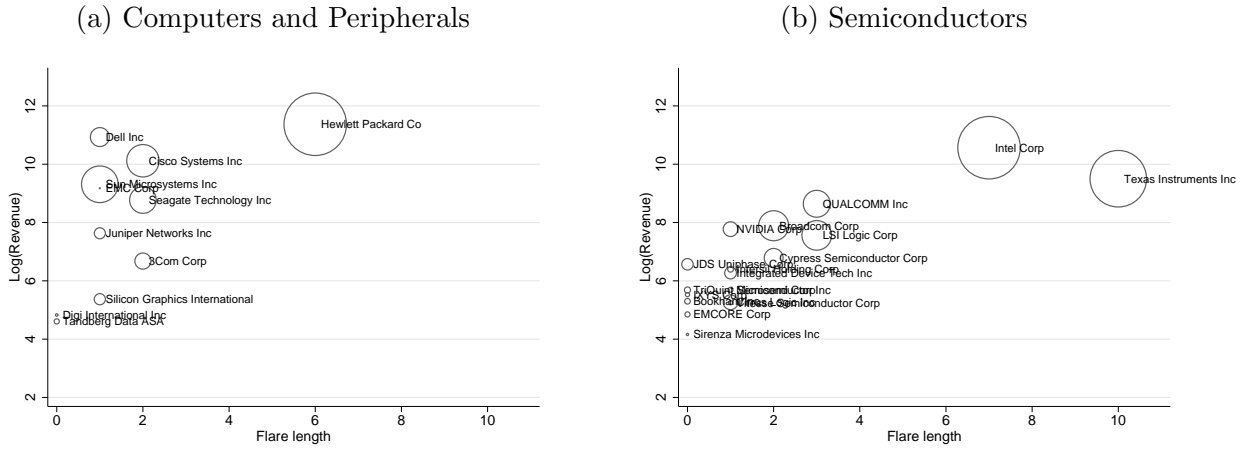
Note: This version uses both R&D and M&A patents, whereas those in Figures 1 and 4 use only R&D patents. Both use log-transform, cosine distance,  $n = 20$ , and  $o = 0.5$ .

Figure 10: Revenues and Flares by Sector



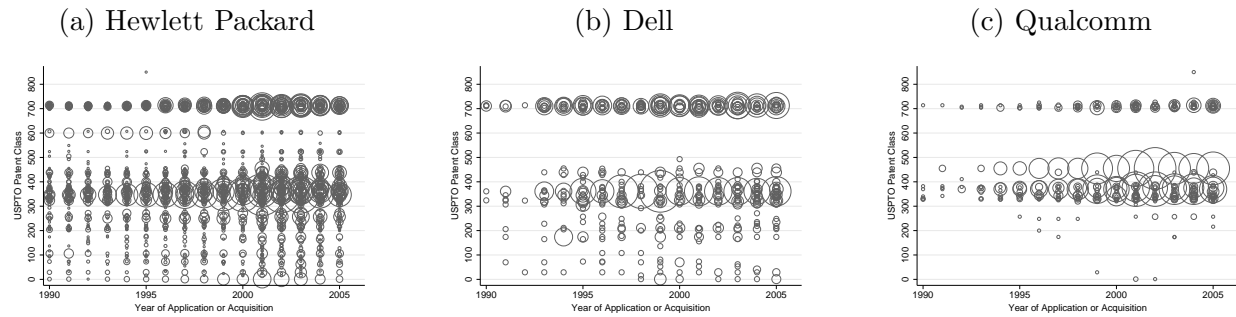
Note: “Consumer goods” include the S&P consumer-cyclicals and consumer-staples sectors. “Others” include the S&P energy, communication services, transport, and utilities sectors.

Figure 11: Revenues and Flares by SIC Code



*Note:* For computers and their peripherals, we use 3570 (computer and office equipment), 3571 (electronic computers), 3572 (computer storage devices), 3575 (computer terminals), and 3576 (computer communications equipment). For semiconductors, we use SIC code 3674 (semiconductors and related devices).

Figure 12: Raw Data on Selected Technology Firms



*Note:* The circle size represents the number of patents in each class-year. The flare lengths of these firms' portfolios are: 6 (HP), 1 (Dell), and 3 (Qualcomm).

Table 6: Flare Regressions Based on Alternative Distance Metrics

LHS variable: Distance metric:	Log(Revenue)			Log(EBIT)			Log(Market value)		
	Euclid (1)	Correl (2)	Min-c (3)	Euclid (4)	Correl (5)	Min-c (6)	Euclid (7)	Correl (8)	Min-c (9)
Constant (= no flare)	6.07 (0.22)	6.07 (0.22)	6.05 (0.22)	3.89 (0.24)	3.96 (0.24)	3.86 (0.24)	6.08 (0.24)	6.17 (0.24)	6.13 (0.24)
Flare length	0.31 (0.08)	0.33 (0.08)	0.28 (0.08)	0.25 (0.08)	0.31 (0.08)	0.21 (0.08)	0.17 (0.08)	0.25 (0.08)	0.19 (0.08)
Islands only	1.04 (1.02)	1.24 (0.73)	1.99 (0.74)	0.71 (1.08)	1.15 (0.77)	1.47 (0.78)	0.16 (1.11)	0.89 (0.79)	1.11 (0.79)
Log(Patents)	0.28 (0.04)	0.28 (0.22)	0.29 (0.04)	0.32 (0.05)	0.30 (0.05)	0.33 (0.05)	0.38 (0.05)	0.35 (0.05)	0.36 (0.05)
$R^2$	.338	.345	.339	.329	.343	.326	.328	.339	.332
Adjusted $R^2$	.332	.339	.333	.322	.336	.320	.322	.333	.326
Number of observations	328	328	328	301	301	301	325	325	325

*Note:* “Euclid,” “correl,” and “min-c” denote Euclidean, correlation, and min-complement distances, respectively. The LHS variables are as of 2005 or the latest years available in Compustat. The RHS variables are based on our topological characterization of the patent statistics between 1976 and 2005. Standard errors are in parentheses.

Table 7: Flares, Counts, and Performances (Survivors through 2005)

LHS variable:	Log(Revenue)			Log(EBIT)			Log(Market value)		
	(1)	(2)	(3)	(4)	(5)	(6)	(7)	(8)	(9)
Constant (= no flare)	7.47 (0.11)	5.66 (0.24)	6.15 (0.26)	5.46 (0.12)	3.62 (0.25)	4.07 (0.27)	8.01 (0.11)	6.11 (0.24)	6.48 (0.27)
Flare length	0.65 (0.07)	— (—)	0.35 (0.08)	0.64 (0.07)	— (—)	0.33 (0.09)	0.61 (0.07)	— (—)	0.26 (0.09)
Islands only	2.49 (1.04)	— (—)	1.17 (1.01)	2.61 (1.11)	— (—)	1.21 (1.08)	2.57 (1.11)	— (—)	1.04 (1.07)
Log(Patents)	— (—)	0.41 (0.04)	0.27 (0.05)	— (—)	0.42 (0.04)	0.29 (0.05)	— (—)	0.42 (0.04)	0.32 (0.05)
$R^2$	.285	.317	.365	.266	.313	.351	.238	.314	.339
Adjusted $R^2$	.279	.314	.357	.260	.310	.343	.232	.311	.332
Number of observations	256	256	256	238	238	238	255	255	255

*Note:* This table is the same as Table 3 except for conditioning on the availability of financial data in 2005.

Table 8: Flares, Counts, and Performances (Balanced Panel, 1976–2005)

LHS variable:	Log(Revenue)			Log(EBIT)			Log(Market value)		
	(1)	(2)	(3)	(4)	(5)	(6)	(7)	(8)	(9)
Constant (= no flare)	8.12 (0.13)	5.76 (0.34)	6.29 (0.38)	5.92 (0.16)	3.52 (0.41)	4.12 (0.46)	8.37 (0.15)	5.71 (0.37)	6.28 (0.42)
Flare length	0.54 (0.07)	— (—)	0.25 (0.08)	0.55 (0.08)	— (—)	0.27 (0.10)	0.58 (0.08)	— (—)	0.26 (0.09)
Islands only	1.39 (1.16)	— (—)	0.10 (1.08)	2.01 (1.38)	— (—)	0.73 (1.32)	2.47 (1.30)	— (—)	0.99 (1.20)
Log(Patents)	— (—)	0.44 (0.05)	0.32 (0.06)	— (—)	0.45 (0.06)	0.32 (0.08)	— (—)	0.50 (0.05)	0.37 (0.07)
$R^2$	.350	.431	.476	.297	.355	.395	.343	.440	.478
Adjusted $R^2$	.338	.425	.462	.284	.349	.378	.331	.435	.463
Number of observations	112	112	112	109	109	109	112	112	112

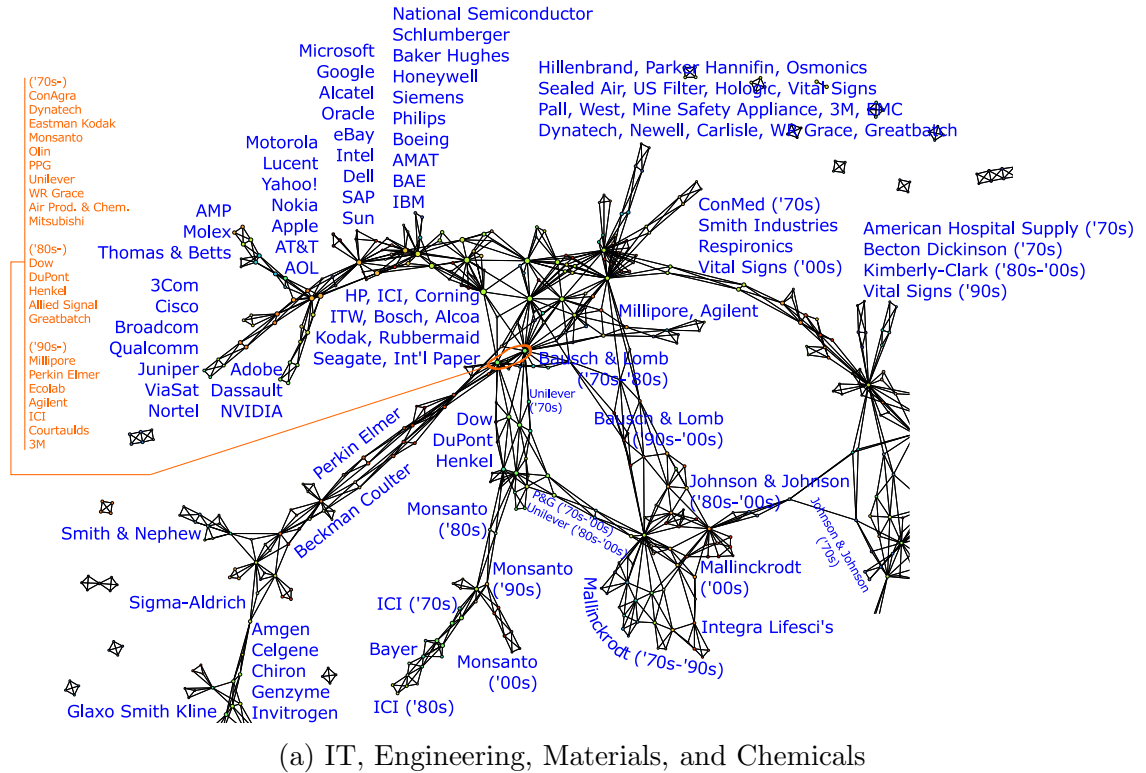
*Note:* This table is the same as Table 3 except for conditioning on the availability of financial data in 1976–2005.

Table 9: K-Means Clustering

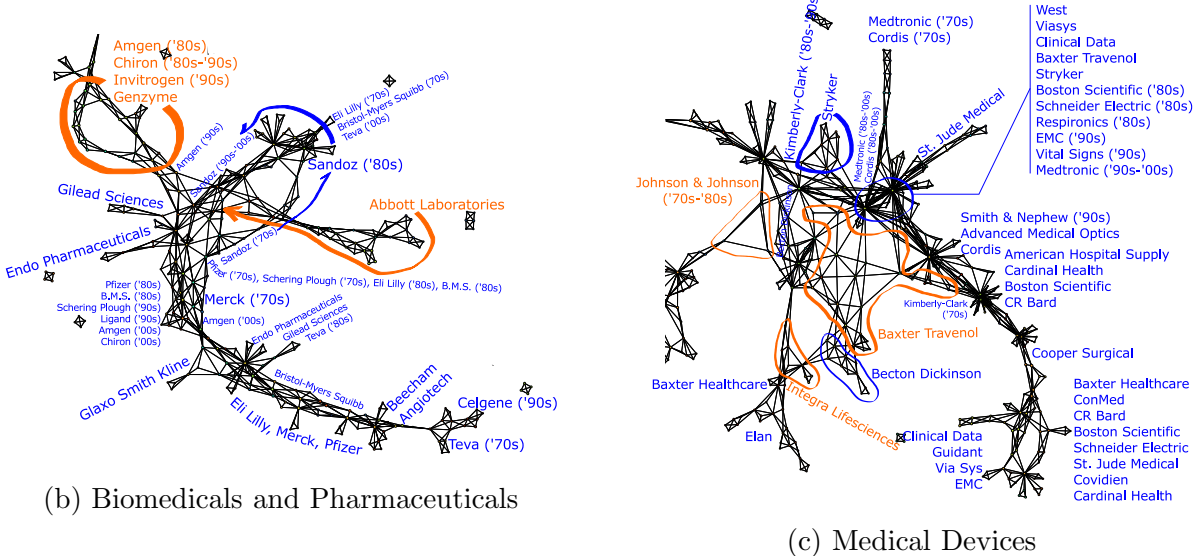
Cluster	Number of firm-years	Number of unique firms	Representative firms
1	5,118	303	(Too many firms to list)
2	438	47	Tellabs, 3Com, Ericsson, Qualcomm, Broadcom
3	421	35	Baxter Travenol, Cordis, C.R.Bard, Medtronic, St. Jude Medical
4	154	19	Amgen, Chiron, Celgene, Genzyme, Invitrogen
5	53	8	BAE Systems, Trimble Navigation, Lockheed Martin
6	44	5	Leggett & Platt, Hillenbrand, Stryker
7	36	9	FLIR Systems, Veeco Instruments, Titan, Lockheed Martin
8	29	4	Federal Signal, Zero
9	18	4	Morgan Crucible, Solelectron, Emhart
10	18	3	Veeco Instruments, Power-One
11	15	4	RPM, Cookson
12	15	4	Roper Industries, Varian
13	15	3	Newell, Carlisle, Avant!
14	12	2	SPS Technologies, Carpenter Technology
15	12	1	Zebra Technologies
16	10	1	Verifone Systems
17	9	2	Carpenter Technology, Lucent
18	8	3	Magne Tek, Franklin Electric
19	5	1	Roper Industries
20	3	2	Terex, Meggitt
21	1	1	Datum
Total	6,434	461	

*Note:* The number of clusters (21) follows Jaffe's original specification. The total number of unique firms exceeds 333, because many firms appear in multiple clusters.

Figure 13: Mapper Graph Based on Jaffe’s Measure (Details)



(a) IT, Engineering, Materials, and Chemicals

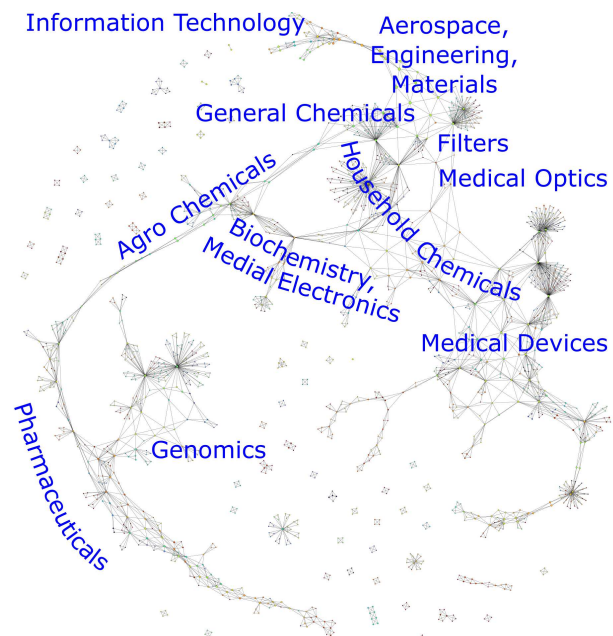


## (b) Biomedicals and Pharmaceuticals

(c) Medical Devices

*Note:* These figures are enlarged and more detailed versions of the Mapper graph in Figure 6.

Figure 14: Mapper Graph Based on Jaffe's Measure and Mahalanobis Distance



*Note:* This is a Mapper graph of 333 major firms' R&D patents in 1976–2005 based on percentage shares, Mahalanobis distance,  $n = 40$ , and  $o = 0.5$ .

## References

Arora, Ashish, Sharon Belenzon, and Lia Sheer (2019). “Matching patents to Compustat firms, 1980-2015: Dynamic reassignment, name changes, and ownership structures”.

Athey, Susan and Guido W Imbens (2017). “The state of applied econometrics: Causality and policy evaluation”. In: *Journal of Economic Perspectives* 31(2), pp. 3–32.

Azoulay, Pierre, Christian Fons-Rosen, and Joshua S. Graff Zivin (Aug. 2019). “Does Science Advance One Funeral at a Time?” In: *American Economic Review* 109(8), pp. 2889–2920.

Bar, Talia and Aija Leiponen (2012). “A measure of technological distance”. In: *Economics Letters* 116(3), pp. 457–459.

Belloni, Alexandre, Victor Chernozhukov, and Christian Hansen (2014). “High-dimensional methods and inference on structural and treatment effects”. In: *Journal of Economic Perspectives* 28(2), pp. 29–50.

Benner, Mary and Joel Waldfogel (2008). “Close to you? Bias and precision in patent-based measures of technological proximity”. In: *Research Policy* 37 (9), pp. 1556–1567.

Bessen, James (2009). “NBER PDP Project User Documentation: Matching Patent Data to Compustat Firms”.

Bloom, Nicholas, Mark Schankerman, and John Van Reenen (2013). “Identifying Technology Spillovers and Product Market Rivalry”. In: *Econometrica* 81(4), pp. 1347–1393.

Brumm, Johannes and Simon Scheidegger (2017). “Using adaptive sparse grids to solve high-dimensional dynamic models”. In: *Econometrica* 85(5), pp. 1575–1612.

Bryan, Kevin A and Yasin Ozcan (2016). “The impact of open access mandates on invention”. In: *Review of Economics and Statistics*, pp. 1–45.

Carlsson, Gunnar (2009). “Topology and data”. In: *Bulletin of the American Mathematical Society* 46(2), pp. 255–308.

Cattaneo, Matias D, Michael Jansson, and Xinwei Ma (2019). “Two-step estimation and inference with possibly many included covariates”. In: *The Review of Economic Studies* 86(3), pp. 1095–1122.

Chazal, Frédéric and Bertrand Michel (2017). “An introduction to Topological Data Analysis: fundamental and practical aspects for data scientists”. In: *arXiv preprint arXiv:1710.04019*.

Chernozhukov, Victor et al. (2018). “Double/debiased machine learning for treatment and structural parameters”. In: *The Econometrics Journal* 21(1), pp. C1–C68.

Cockburn, Iain M, Jean O Lanjouw, and Mark Schankerman (2016). “Patents and the global diffusion of new drugs”. In: *American Economic Review* 106(1), pp. 136–64.

Cohen, Wesley M. (2010). "Fifty Years of Empirical Studies of Innovative Activity and Performance". In: *Handbook of the Economics of Innovation*. Ed. by Bronwyn H. Hall and Nathan Rosenberg. Vol. 1. Elsevier, pp. 129–213.

Edelsbrunner, Herbert and John Harer (2010). *Computational topology: an introduction*. American Mathematical Society.

Edelsbrunner, Herbert, David Letscher, and Afra Zomorodian (2000). "Topological persistence and simplification". In: *Proceedings 41st Annual Symposium on Foundations of Computer Science*. IEEE, pp. 454–463.

Epstein, Charles, Gunnar Carlsson, and Herbert Edelsbrunner (2011). "Topological data analysis". In: *Inverse Problems* 27(12), p. 120201.

European Commission (2017). *CASE M.7932 - Dow/DuPont*.

Gentzkow, Matthew, Bryan Kelly, and Matt Taddy (2019). "Text as data". In: *Journal of Economic Literature* 57(3), pp. 535–74.

Gidea, Marian (2017). "Topological Data Analysis of Critical Transitions in Financial Networks". In: *3rd International Winter School and Conference on Network Science*. Ed. by Erez Shmueli, Baruch Barzel, and Rami Puzis. Springer International Publishing: Cham, pp. 47–59.

Gidea, Marian and Yuri Katz (2018). "Topological data analysis of financial time series: Landscapes of crashes". In: *Physica A: Statistical Mechanics and its Applications* 491, pp. 820–834.

Goel, Anubha, Puneet Pasricha, and Aparna Mehra (2020). "Topological data analysis in investment decisions". In: *Expert Systems with Applications* 147, p. 113222.

Griliches, Zvi (1990). "Patent Statistics as Economic Indicators: A Survey". In: *Journal of Economic Literature* 28(4), pp. 1661–1707.

Guo, Hongfeng et al. (2020). "Empirical study of financial crises based on topological data analysis". In: *Physica A: Statistical Mechanics and its Applications* 558, p. 124956.

Hall, Bronwyn, Adam Jaffe, and Manuel Trajtenberg (2001). *The NBER patent citation data file: Lessons, insights and methodological tools*. Tech. rep. National Bureau of Economic Research.

Hall, Bronwyn, Adam Jaffe, and Manuel Trajtenberg (2005). "Market value and patent citations". In: *RAND Journal of economics*, pp. 16–38.

Hiraoka, Yasuaki et al. (2016). "Hierarchical structures of amorphous solids characterized by persistent homology". In: *Proceedings of the National Academy of Sciences of the United States of America* 113(26), pp. 7035–7040.

Hoberg, Gerard and Gordon Phillips (2016). “Text-based network industries and endogenous product differentiation”. In: *Journal of Political Economy* 124(5), pp. 1423–1465.

Howell, Sabrina T (2017). “Financing innovation: Evidence from R&D grants”. In: *American Economic Review* 107(4), pp. 1136–64.

Igami, Mitsuru (2020). “Artificial intelligence as structural estimation: Deep Blue, Bonanza, and AlphaGo”. In: *Econometrics Journal* 23(3), S1–S24.

Igami, Mitsuru and Jai Subrahmanyam (2019). “Patent Statistics as an Innovation Indicator? Evidence from the Hard Disk Drive Industry”. In: *Japanese Economic Review* 70(3), pp. 308–330.

Iskhakov, Fedor, John Rust, and Bertel Schjerning (2020). “Machine Learning and Structural Econometrics: Contrasts and Synergies”. In: *Econometrics Journal*.

Jaffe, Adam (1989). “Characterizing the “technological position” of firms, with application to quantifying technological opportunity and research spillovers”. In: *Research Policy* 18(2), pp. 87–97.

Jaffe, Adam, Manuel Trajtenberg, and Rebecca Henderson (1993). “Geographic Localization of Knowledge Spillovers as Evidenced by Patent Citations”. In: *Quarterly Journal of Economics* 108(3), pp. 577–598.

Kuhn, Jeffrey, Kenneth Younge, and Alan Marco (2020). “Patent citations reexamined”. In: *The RAND Journal of Economics* 51(1), pp. 109–132.

Lerner, Josh and Amit Seru (2017). “The Use and Misuse of Patent Data: Issues for Corporate Finance and Beyond”. In: *NBER Working Paper 24053*.

Lerner, Josh and Scott Stern (2012). “Introduction”. In: *The Rate and Direction of Inventive Activity Revisited*. Ed. by Josh Lerner and Scott Stern. University of Chicago Press: Chicago, IL.

Lum, Pek Y et al. (2013). “Extracting insights from the shape of complex data using topology”. In: *Scientific reports* 3, p. 1236.

Majumdar, Sourav and Arnab Kumar Laha (2020). “Clustering and classification of time series using topological data analysis with applications to finance”. In: *Expert Systems with Applications*, p. 113868.

Moser, Petra and Shmuel San (2020). *Immigration, Science, and Invention. Evidence from the Quota Acts*. Tech. rep.

Myers, Kyle (2020). “The Elasticity of Science”. In: *American Economic Journal: Applied Economics*.

Myers, Kyle and Lauren Lanahan (2020). “Research Subsidy Spillovers, Two Ways”.

Nagaoka, Sadao, Kazuyuki Motohashi, and Akira Goto (2010). “Patent Statistics as an Innovation Indicator”. In: *Handbook of the Economics of Innovation*. Ed. by Bronwyn H. Hall and Nathan Rosenberg. Vol. 2. Elsevier, pp. 1083–1127.

Nelson, Richard (1962). “Introduction”. In: *The Rate and Direction of Inventive Activity: Economic and Social Factors*. Ed. by Committee on Economic Growth of the Social Science Research Council Universities-National Bureau Committee for Economic Research. Princeton University Press: Princeton, NJ.

Nicolau, Monica, Arnold J Levine, and Gunnar Carlsson (2011). “Topology based data analysis identifies a subgroup of breast cancers with a unique mutational profile and excellent survival”. In: *Proceedings of the National Academy of Sciences* 108(17), pp. 7265–7270.

Ozcan, Yasin (2015). “Innovation and Acquisition: Two-Sided Matching in M&A Markets”.

Pakes, Ariel and Zvi Griliches (1984). “Patents and R&D at the Firm Level: A First Look”. In: *R&D, Patents and Productivity*. Ed. by Zvi Griliches. University of Chicago Press: Chicago, Illinois.

Qiu, Wanling, Simon Rudkin, and Paweł Dłotko (2020). “Refining understanding of corporate failure through a topological data analysis mapping of Altman’s Z-score model”. In: *Expert Systems with Applications* 156, p. 113475.

Rizvi, Abbas H et al. (2017). “Single-cell topological RNA-seq analysis reveals insights into cellular differentiation and development”. In: *Nature biotechnology* 35(6), p. 551.

Saggar, Manish et al. (2018). “Towards a new approach to reveal dynamical organization of the brain using topological data analysis”. In: *Nature communications* 9(1), pp. 1–14.

Sampat, Bhaven and Heidi L Williams (2019). “How do patents affect follow-on innovation? Evidence from the human genome”. In: *American Economic Review* 109(1), pp. 203–36.

Singh, Gurjeet, Facundo Mémoli, and Gunnar Carlsson (2007). “Topological methods for the analysis of high dimensional data sets and 3d object recognition.” In: *SPBG*, pp. 91–100.

Sizemore, Ann E. et al. (2019). “The importance of the whole: Topological data analysis for the network neuroscientist”. In: *Network Neuroscience* 3(3), pp. 656–673.

Tukey, John Wilder (1977). *Exploratory Data Analysis*. Addison-Wesley.

Van Veen, Hendrik Jacob and Nathaniel Saul (2019). *KeplerMapper*. URL: <http://doi.org/10.5281/zenod0>

Varian, Hal R (2014). “Big data: New tricks for econometrics”. In: *Journal of Economic Perspectives* 28(2), pp. 3–28.

Yao, Yuan et al. (2009). “Topological methods for exploring low-density states in biomolecular folding pathways”. In: *The Journal of chemical physics* 130(14), 04B614.

Zomorodian, Afra and Gunnar Carlsson (2005). “Computing persistent homology”. In: *Discrete & Computational Geometry* 33(2), pp. 249–274.